

## **Chapter 2**

# **Fatigue as a Phenomenon in the Material**

- 2.1 Introduction
  - 2.2 Different phases of the fatigue life
  - 2.3 Crack initiation
  - 2.4 Crack growth
  - 2.5 The fatigue mechanism in more detail
    - 2.5.1 Crystallographic nature of the material
    - 2.5.2 Crack initiation at inclusions
    - 2.5.3 Small cracks, crack growth barriers, thresholds
    - 2.5.4 Number of crack nuclei
    - 2.5.5 Surface effects
    - 2.5.6 Crack growth and striations
    - 2.5.7 Environmental effects
    - 2.5.8 Cyclic tension and cyclic torsion
  - 2.6 Characteristic features of fatigue failures
    - 2.6.1. Microscopic characteristics
    - 2.6.2. Macroscopic characteristics
  - 2.7 Main topics of the present chapter
- References

## **2.1 Introduction**

In a specimen subjected to a cyclic load, a fatigue crack nucleus can be initiated on a microscopically small scale, followed by crack grows to a macroscopic size, and finally to specimen failure in the last cycle of the fatigue life. In the present chapter the fatigue phenomenon will be discussed as a mechanism occurring in metallic materials, first on a microscale and later on a macroscale.

Understanding of the fatigue mechanism is essential for considering various technical conditions which affect fatigue life and fatigue crack

growth, such as the material surface quality, residual stress, and environmental influence. This knowledge is essential for the analysis of fatigue properties of an engineering structure. Fatigue prediction methods can only be evaluated if fatigue is understood as a crack initiation process followed by a crack growth period. For that reason, the present chapter is a prerequisite for most chapters of this book.

The fatigue life is usually split into a *crack initiation period* and a *crack growth period*. The initiation period is supposed to include some microcrack growth, but the fatigue cracks are still too small to be visible. In the second period, the crack is growing until complete failure. It is technically significant to consider the crack initiation and crack growth periods separately because several practical conditions have a large influence on the crack initiation period, but a limited influence or no influence at all on the crack growth period. This chapter starts with a general definition of the fatigue life as consisting of different phases (Section 2.2). Crack initiation and growth are then described as different phenomena (Sections 2.3 and 2.4). In order to understand the effects of the variables, the fatigue mechanism is considered in more detail in Section 2.5. It also covers the basics of several variables which are discussed as technical problems in later chapters. Characteristic features of fatigue failures are summarized in Section 2.6. The major concepts developed in this chapter are summarized in the final section, Section 2.7.

## 2.2 Different phases of the fatigue life

Microscopic investigations in the beginning of the 20th century [1] have shown that fatigue crack nuclei start as invisible microcracks in slip bands. After more microscopic information on the growth of small cracks became available, it turned out that nucleation of microcracks generally occurs very early in the fatigue life. Indications were obtained that it may take place almost immediately if a cyclic stress above the fatigue limit is applied. The fatigue limit is the cyclic stress level below which a fatigue failure does not occur.<sup>3</sup> In spite of early crack nucleation, microcracks remain invisible for a considerable part of the total fatigue life. Once cracks become visible, the remaining fatigue life of a laboratory specimen is usually a small percentage

---

<sup>3</sup> The fatigue limit depends on the mean stress of the cyclic load, but for clarity of the text, this will be disregarded if it does not affect the discussion.

of the total life. The latter percentage may be much larger for real structures such as ships, aircraft, etc.

After a microcrack has been nucleated, crack growth can still be a slow and erratic process, due to effects of the microstructures, e.g. grain boundaries. However, after some microcrack growth has occurred away from the nucleation site, a more regular growth is observed. This is the beginning of the real crack growth period. Various steps in the fatigue life are indicated in Figure 2.1. The important point is that the fatigue life until failure consists of two periods: the *crack initiation period* and the *crack growth period*. Differentiating between the two periods is of great importance because several surface conditions do affect the initiation period, but have a negligible influence on the crack growth period. Surface roughness is just one of those conditions as discussed in Section 2.5. Corrosive environments can affect initiation and crack growth, but in a different way for the two periods. Differences between the crack initiation period and crack growth period are discussed in Sections 2.3 and 2.4. It should already be noted here that fatigue prediction methods are different for the two periods. The stress concentration factor  $K_t$  is the important parameter for predictions on crack initiation. The stress intensity factor  $K$  is used for predictions on crack growth. These two parameters are discussed in Chapters 3 and 5 respectively.

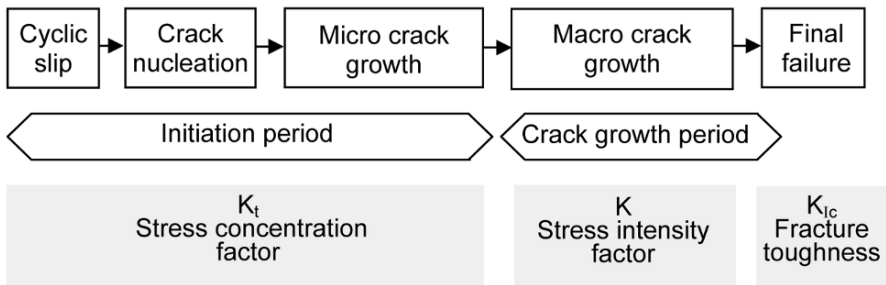


Fig. 2.1 Different phases of the fatigue life and relevant factors.

### 2.3 Crack initiation

Fatigue crack initiation and crack growth are a consequence of cyclic slip. It implies cyclic plastic deformation, or in other words dislocation activities. Fatigue occurs at stress amplitudes below the yield stress. At such a low

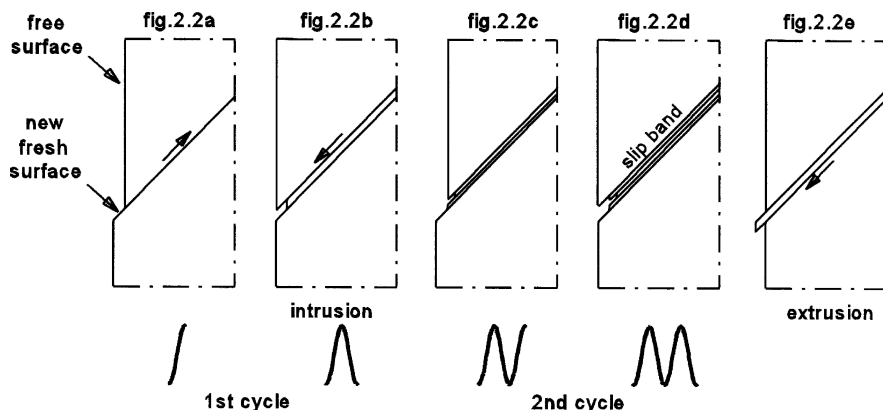
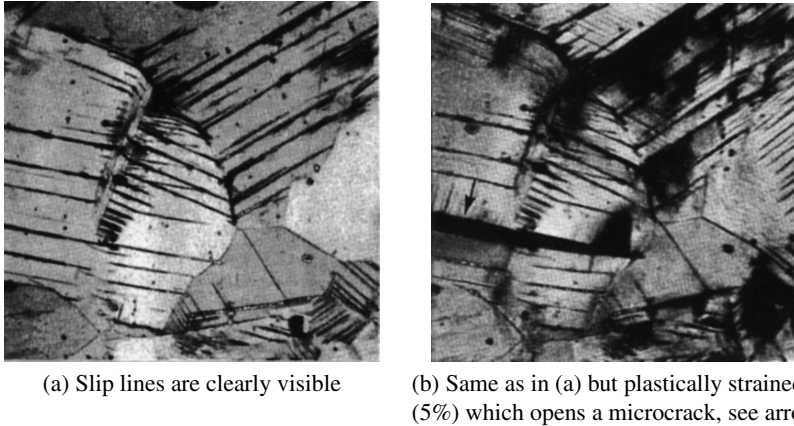


Fig. 2.2 Cycle slip leads to crack nucleation.

stress level, plastic deformation is limited to a small number of grains of the material. This microplasticity preferably occurs in grains at the material surface because of the lower constraint on slip. At the free surface of a material, the surrounding material is present on one side only. The other side is the environment, usually a gaseous environment (e.g. air) or a liquid (e.g. sea water). As a consequence, plastic deformation in surface grains is less constrained by neighbouring grains than in subsurface grains; it can occur at a lower stress level.

Cyclic slip requires a cyclic shear stress. On a microscale the shear stress is not homogeneously distributed through the material. The shear stress on crystallographic slip planes differs from grain to grain, depending on the size and shape of the grains, crystallographic orientation of the grains, and elastic anisotropy of the material. In some grains at the material surface, these conditions are more favorable for cyclic slip than in other surface grains. If slip occurs in a grain, a slip step will be created at the material surface, see Figure 2.2a. A slip step implies that a rim of new material will be exposed to the environment. The fresh surface material will be immediately covered by an oxide layer in most environments, at least for most structural materials. Such monolayers strongly adhere to the material surface and are not easily removed. Another significant aspect is that slip during the increase of the load also implies some strain hardening in the slip band. As a consequence, upon unloading (Figure 2.2b) a larger shear stress will be present on the same slip band, but now in the reversed direction. Reversed slip will thus preferably occur in the same slip band. If fatigue would be a fully reversible process, this book would not have been written. However,



**Fig. 2.3** Development of cyclic slip bands and a microcrack in a pure copper specimen.  $S_m = 0$ ,  $S_a = 77.5$  MPa,  $N = 2 \times 10^6$  [2].

we have already mentioned two reasons why it cannot be fully reversible. First, the oxide monolayer cannot simply be removed from the slip step. Secondly, strain hardening in the slip band is also not fully reversible. As a consequence, reversed slip, although occurring in the same slip band, will occur on adjacent parallel slip planes. This is schematically indicated in Figure 2.2b. The same sequence of events can occur in the second cycle, see Figures 2.2c and d.

Of course Figure 2.2 offers a simplified picture, but there are still some important lessons to be learned:

- (i) A single cycle is sufficient to create a microscopical intrusion into the material, which in fact is a microcrack.
- (ii) The mechanism occurring in the first cycle can be repeated in the second cycle, and in subsequent cycles and cause crack extension in each cycle.
- (iii) The first initiation of a microcrack may well be expected to occur along a slip band. This has been confirmed by several microscopic investigations, see Figure 2.3. A slip band seen in Figure 2.3a is actually a microcrack as confirmed in Figure 2.3b after the band is opened by applying a 5% plastic strain to the material. A part of this slip band was already visible after no more than 0.5% of the fatigue life.
- (iv) In Figure 2.2 the small shift of the slip planes during loading and unloading is leading to an intrusion. However, if the reversed slip would occur at the lower side of the slip band, an extrusion is obtained, see Figure 2.2e. Such extrusions have been reported in the literature, noteworthy by Forsyth [3]. However, from a potential strain energy

point of view, the intrusion is the more probable consequence of cyclic slip in a slip band.<sup>4</sup>

- (v) The simple mechanism of Figure 2.2, and even if it would be different or more complicated, implies disruption of bonds between atoms, i.e. *decohesion* occurs, either by tensile decohesion, shear decohesion, or both. It occurs if a slip step penetrates through a free surface. It can also occur at the tip of a growing fatigue crack. The disruption of bonds at the crack tip might also be caused by a generation of dislocations from the crack tip. It should be expected that the decohesion can be accelerated by an aggressive environment.

The lower restraint on cyclic slip at the material surface has been mentioned as a favorable condition for crack initiation at the free surface. However, more arguments for crack initiation at the material surface are present. A very practical reason is the inhomogeneous stress distribution due to a notch effect of a hole or some other geometric discontinuity. Because of an inhomogeneous stress distribution, a peak stress occurs at the surface (stress concentration). Furthermore, surface roughness also promotes crack initiation at the material surface. Other surface conditions with a similar effect are corrosion pits and fretting fatigue damage both occurring at the material surface. These technical conditions are discussed later. The most important conclusion to be drawn here is:

*In the crack initiation period, fatigue is a material surface phenomenon.*

## 2.4 Crack growth

As long as the size of the microcrack is still in the order of a single grain, the microcrack is obviously present in an elastically anisotropic material with a crystalline structure and a number of different slip systems. The microcrack contributes to an inhomogeneous stress distribution on a microlevel, with

---

<sup>4</sup> The author has found extrusions in slip bands of the pure aluminium cladding layer of 2024-T3 aluminium alloy sheet material. Under cyclic loading plastic shake down will occur in this soft layer. It implies that it will also see compressive stresses even if the nominal stress on the sheet material is cyclic tension. Under compression the extrusion mechanism should be favored.

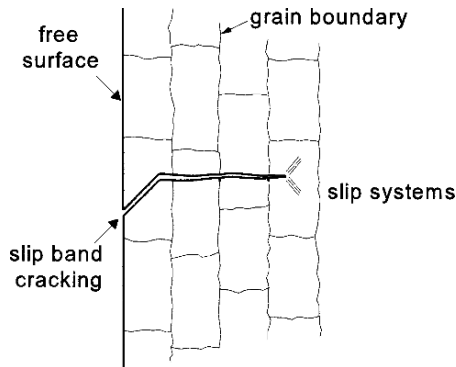


**Fig. 2.4** Cross section of microcrack.

a stress concentration at the tip of the microcrack. As a result, more than one slip system may be activated. Moreover, if the crack is growing into the material in some adjacent grains, the constraint on slip displacements will increase due to the presence of the neighbouring grains. Similarly, it will become increasingly difficult to accommodate the slip displacements by slip on one slip plane only. It should occur on more slip planes. The microcrack growth direction will then deviate from the initial slip band orientation. In general, there is a tendency to grow perpendicular to the loading direction, see Figure 2.4.

Because microcrack growth is depending on cyclic plasticity, barriers to slip can imply a threshold for crack growth. This has been observed indeed. Illustrative results are presented in Figure 2.5. The crack growth rate measured as the crack length increment per cycle decreased when the crack tip approached the first grain boundary. After penetrating through the grain boundary the crack growth rate increased during growth into the next grain, but it decreased again when approaching the second grain boundary. After passing that grain boundary, the microcrack continued to grow with a steadily increasing rate.

In the literature, several observations are reported on initially inhomogeneous microcrack growth, which starts with a relatively high crack growth rate and then slows down or even stops due to material structural barriers. However, the picture becomes different if the crack front after some crack growth passes through a substantial number of grains, as schematically indicated in Figure 2.6. Because the crack front must remain a coherent crack front, the crack cannot grow in each grain in an arbitrary direction and at any growth rate independent of crack growth in the adjacent grains. This continuity prevents large gradients of the crack growth rate along the

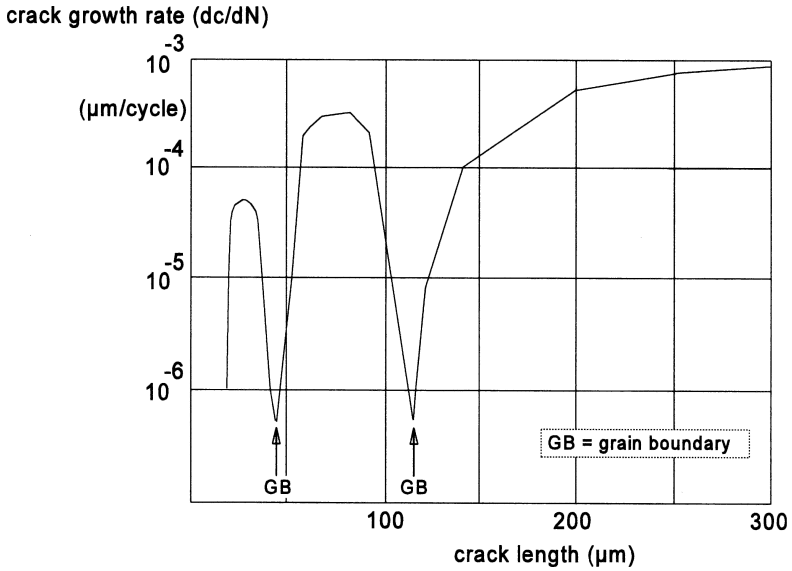


Fig. 2.5 Grain boundary effect on crack growth in an Al-alloy [4]. The crack length was measured along the material surface.

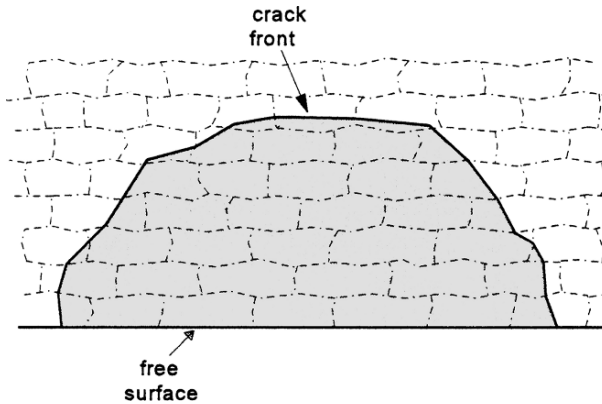


Fig. 2.6 Top view of crack with crack front passing through many grains.

crack front. As soon as the number of grains along the crack front becomes sufficiently large, crack growth occurs as a more or less continuous process along the entire crack front. The crack front can be approximated by a continuous line, which could have a semi-elliptical shape. How fast the crack will grow depends on the crack growth resistance of the material. Two important surface aspects are no longer relevant. The lower restraint on cyclic slip at the surface is not applicable at the interior of the material. Secondly,

surface roughness and other surface conditions do not affect crack growth. This leads to the second important conclusion:

*Crack growth resistance when the crack penetrates into the material depends on the material as a bulk property. Crack growth is no longer a surface phenomenon.*

## 2.5 The fatigue mechanism in more detail

In the previous section, the fatigue life was discussed as consisting of a crack initiation period and crack growth period. The transition from the initiation period to the crack growth period has not yet been defined. The definition cannot really be given in quantitative terms, but in a qualitative way the following definition will be used:

*The initiation period is supposed to be completed when microcrack growth is no longer depending on the material surface conditions.*

It implies that the crack growth period starts if the crack growth resistance of the material per se is controlling the crack growth rate. The size of the microcrack at the transition from the initiation period to the crack growth period can be significantly different for different types of materials. The transition depends on microstructural barriers to be overcome by a growing microcrack, and these barriers are not the same in all materials.

The crack initiation period includes the initial microcrack growth. Because the growth rate is still low, the initiation period may cover a significant part of the fatigue life. This is illustrated by the generalized picture of crack growth curves presented in Figure 2.7 which schematically shows the crack growth development as a function of the percentage of the fatigue life consumed ( $= n/N$ ), with  $n$  as the number of fatigue cycles and  $N$  as the fatigue life until failure. Complete failure corresponds to  $n/N = 1 = 100\%$ . There are three curves in Figure 2.7, all of them in agreement with crack initiation in the very beginning of the fatigue life, however, with different values of the initial crack length. The lower curve

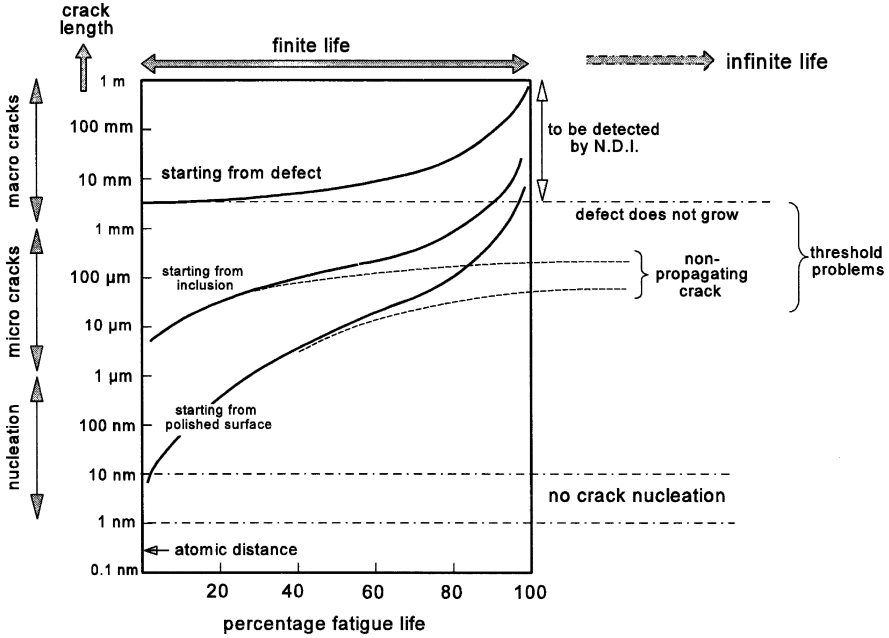


Fig. 2.7 Different scenarios of fatigue crack growth.

corresponds to microcrack initiation at a “perfect” surface of the material. Here, the mechanism of Figure 2.2 could be applicable. The middle curve represents crack initiation from an inclusion, which is briefly discussed later. The upper curve is associated with a crack starting from a material defect which should not have been present, such as defects in a welded joint. Figure 2.7 illustrates some interesting aspects:

- (i) The vertical crack length scale is a logarithmic scale, ranging from 0.1 nanometer (nm) to 1 meter (1 nanometer =  $10^{-9}$  m =  $4 \cdot 10^{-8}$  inch). Microcracks starting from a perfect free surface can have a sub-micron crack length ( $<1 \mu\text{m} = 10^{-6}$  m). However, cracks nucleated at an inclusion will start with a size similar to the size of the inclusion. The size can still be in the sub-millimeter range. Only cracks starting from macrodefects can have a detectable macrocrack length immediately.
- (ii) The two lower crack growth curves illustrate that the major part of the fatigue life is spent with a crack size below 1 mm, i.e. with a practically invisible crack size.
- (iii) Dotted lines in Figure 2.7 indicate the possibility that cracks do not always grow until failure. It implies that there must have been barriers in the material which stopped crack growth.

Figure 2.7 gives generalized scenarios about possible crack growth developments. In order to understand more about fatigue under various practical conditions, several aspects of the fatigue mechanism are discussed in more detail. The aspects covered in this section are:

1. Crystallographic nature of the material;
2. Crack initiation at inclusions;
3. Small cracks, crack growth barriers, crack growth thresholds;
4. Number of crack nuclei;
5. Surface effects;
6. Macrocrack growth and striations;
7. Environmental effects;
8. Cyclic tension and cyclic torsion.

### ***2.5.1 Crystallographic aspects***

As pointed out before, the initial growth of a microcrack shows a tendency to grow along a slip band. It thus must be expected that the crystallography of a material has some influence on the mechanistic behavior during the initiation period. The crystallographic properties vary from one material to another. As a consequence, the initial microcracking depends on the material. Aspects to be mentioned here are:

- Type of crystal lattice, elastic anisotropy, allotropy;
- Slip systems, ease of cross slip;
- Grain size and shape;
- Variation of the crystal orientation from grain to grain (texture).

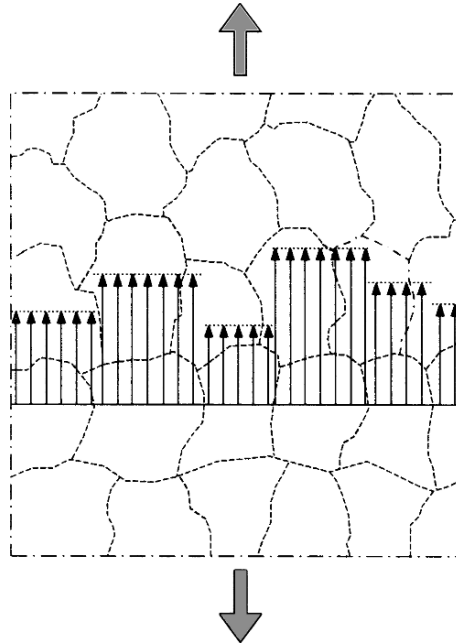
These subjects will not be discussed extensively, but some significant features are reviewed for understanding differences between the fatigue mechanisms in different materials, especially so for the crack initiation period, i.e. for small microcracks.

The three well-known crystal lattices are face centered cubic (f.c.c.) for Al, Cu, Ni and  $\gamma$ -Fe, body centered cubic (b.c.c.) for  $\alpha$ -Fe and  $\beta$ -Ti, and hexagonal close packed (h.c.p.) for  $\alpha$ -Ti and Mg. The elastic and plastic behavior of a material depends on the crystal structure, but even for the same crystal lattice large differences can occur. The elastic anisotropy can vary considerably as illustrated by the  $E$ -moduli in Table 2.1.

The anisotropy is quite large for copper and fairly small for Al, with  $\alpha$ -Fe (ferrite) at an intermediate position. Fatigue generally occurs at low stress

**Table 2.1** Some data on elastic anisotropy.

Material	$E_{\max}$ [111] (MPa)	$E_{\min}$ [100] (MPa)	Ratio max/min
$\alpha$ -Fe	284500	132400	2.15
Al	75500	62800	1.20
Cu	190300	66700	2.85

**Fig. 2.8** Simplified picture of the inhomogeneous stress distribution from grain to grain due to elastic anisotropy.

levels without macroplastic deformation. As a result of the elastic anisotropy, the stress distribution from grain to grain should be inhomogeneous as schematically indicated in Figure 2.8. Such a picture suggests a homogeneous stress in each single grain, which is an approximation. However, one conclusion remains valid. The inhomogeneity of the stress distribution from grain to grain are small for Al-alloys and much larger for steel. In other words, in Al-alloys most grains will be subjected to similar stress levels, whereas for steel and other materials the stress level can vary significantly from grain to grain.

Slip systems are characterized by crystallographic planes on which slip occurs and by crystallographic slip directions. Slip systems have been

extensively studied and are well documented in textbooks on material science. The possibility of cross slip is important for dislocation movements in order to circumvent obstacles and to continue slip on adjacent parallel slip planes. Cross slip is easier if the stacking fault energy of a material is high, and difficult if the stacking fault energy is low. Aluminium is a noteworthy example for easy cross slip and nickel for difficult cross slip. As a result, slip lines in Al are wavy and cyclic slip can lead to slip bands with a measurable thickness. In Ni- and Cu-alloys, slip lines are more sharply defined straight lines, see as an example Figure 2.3. Moreover, if the number of easily activated slip systems is limited, microcracks persist much longer in growing along crystallographic directions. This behavior may continue until a crack length in the order of 1 mm (0.04 inch), while for Al-alloys cracks as small as 0.1 mm already grow more or less perpendicular to the main principal stress, usually the tensile stress along the material surface. Such observations show that the microcrack growth behavior can be essentially different for different types of material.

### ***2.5.2 Crack initiation at inclusions***

In most technical materials, a variety of inclusions can be present, such as impurities introduced during the melting production process of the alloys. In the present section, inclusions of a microscopic size are considered. Larger macroscopic inclusions are generally regarded as material defects which should not be present, for example slag streaks, weld defects, major porosities. Large defects have occasionally caused disastrous failures in service, but they are not considered in this section.

Non-metallic inclusions of a microscopic size (10 to 100  $\mu\text{m}$ ) have been observed in low-alloy high-strength steels. Fatigue crack nucleation occurred at these inclusions located at the material surface or slightly below the surface. Crack nucleation can occur in aluminium alloys at intermetallic inclusions which partially contain alloying elements. These inclusions are not considered to be harmful for the static strength, but the inclusions can reduce the ductility of a material due to generating internal voids at large plastic strains. However, significant plasticity does not occur under fatigue at a relatively low stress level. But the inclusions are still foreign constituents which can interact with cyclic slip. The inclusions affect the stress distribution on a microlevel and thus can contribute to crack

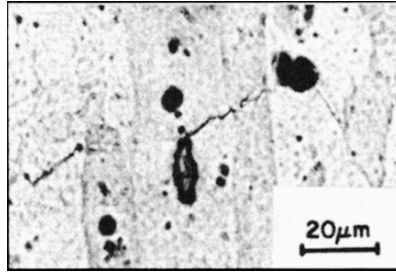


**Fig. 2.9** Slip band microcrack nucleated at the tip of an intermetallic inclusion in the polished material surface of an aluminium alloy (2024-T3) specimen [7].

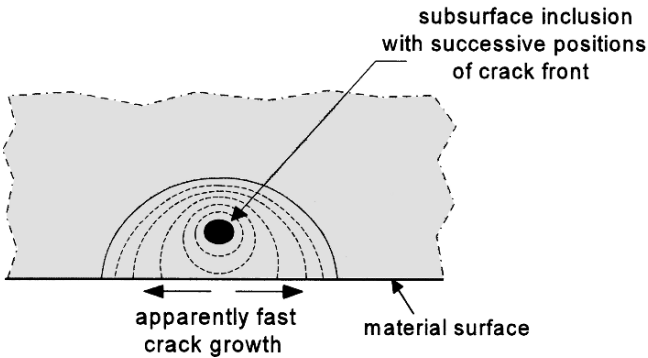


**Fig. 2.10** Subsurface nucleation of fatigue crack at inclusion which suggests initial fast crack growth [8].

nucleation. Nucleation starting from inclusions has been shown in several publications, see e.g. [5, 6]. An example is shown in Figure 2.9.

The nucleation of a microcrack at an inclusion can occur slightly subsurface and not necessarily at the material surface. However, the free surface argument (lower restraint on slip) remains valid. It is for this reason that crack nucleation far below the material surface is rarely observed, although it can occur if the inclusion is large, or if a residual tensile stress is present away from the material surface.

An interesting situation arises if a microcrack initiated at a subsurface inclusion penetrates through the ligament between the inclusion and the free surface, see Figure 2.10. Crack growth observed on the material surface corresponds to a kind of a *break-through*. As a result, an initially high growth rate is observed which slows down later when the crack becomes a true surface crack. This is another reason for an apparently unsystematic development of the crack growth rate in the crack initiation period.

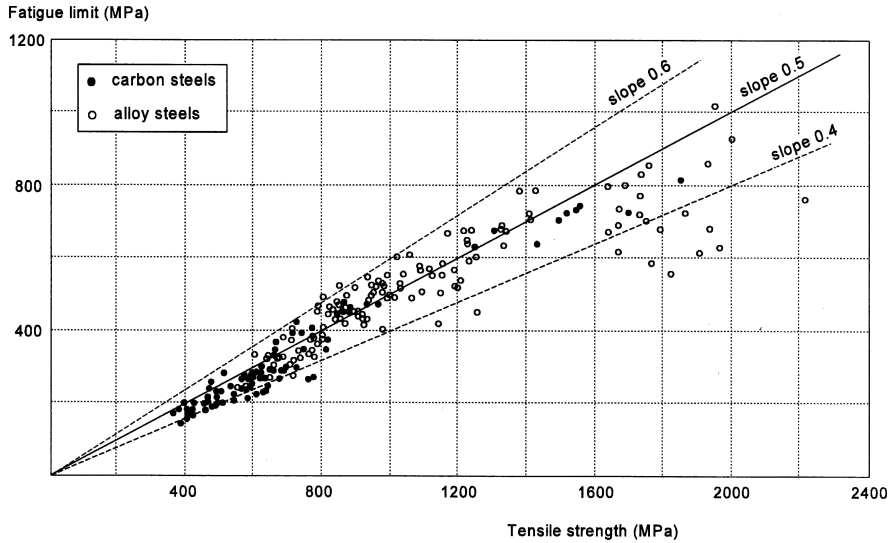


Fig. 2.11 The fatigue limit of steels as a function of the ultimate tensile strength [9].

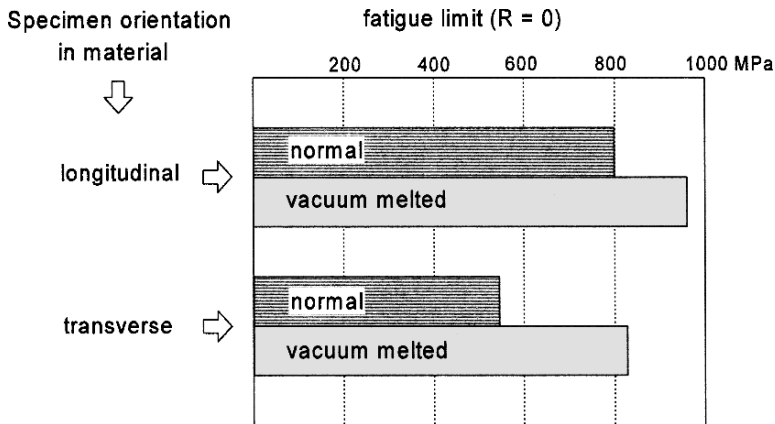
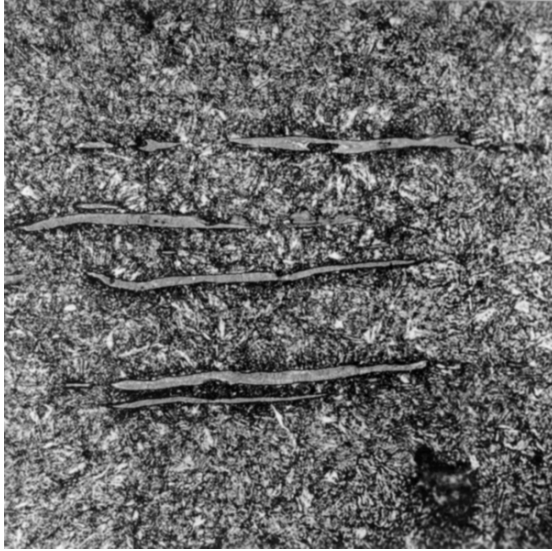


Fig. 2.12 The influence of inclusions on the fatigue limit of a high-strength steel (SAE 4340) [10].

The significance of inclusions for fatigue in steel has received considerable interest in the past. It was observed that the fatigue limit of different types of steel increased approximately proportionally to the tensile strength, see Figure 2.11. However, at very high values of the tensile strength, this trend was not continued and lower fatigue limits were obtained. The explanation was found by considering inclusions in high-strength steel. The inclusions act as micronotches in the material which can generate



**Fig. 2.13** Non-metallic slag inclusions in a martensitic matrix of a high-strength steel. (Courtesy H.P. van Leeuwen, NLR, Amsterdam)

fatigue crack nuclei, especially in high-strength material. Because of the high-yield stress of these materials they have a high notch sensitivity, even for micronotches. In low-strength steels, inclusions are less harmful because of the lower notch-sensitivity. Improvements of the fatigue limit of high-strength steels could be obtained by purifying the composition to eliminate inclusions. The improvement is illustrated by the results in Figure 2.12 for a high-strength NiCrMo steel. It is noteworthy that the fatigue limit of the “normal” material shows a significant anisotropy. Specimens in the transverse direction have a 32% lower fatigue limit than in the longitudinal direction. This is due to the directionality of the elongated inclusions with the long dimension in the longitudinal direction. An example of such inclusions from another investigation is shown in Figure 2.13. After a vacuum melting process, the number of inclusions is drastically reduced, which increases the fatigue limit considerably and at the same time the directionality effect is also smaller as illustrated by the data in Figure 2.12.

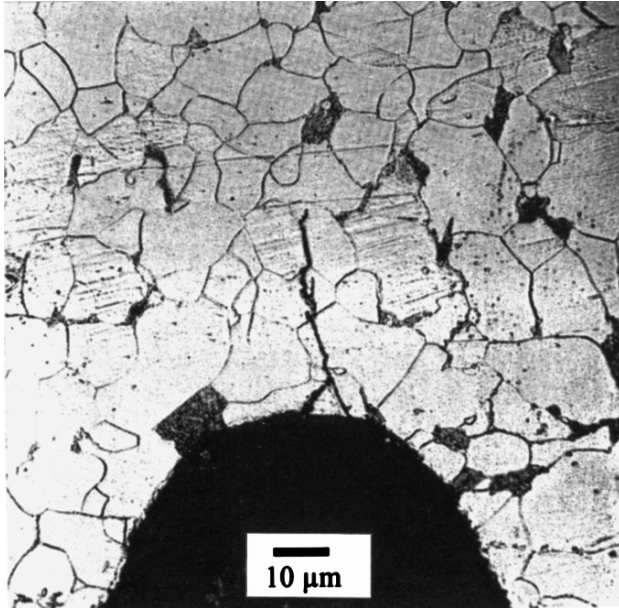


**Fig. 2.14** Non-propagating fatigue crack at the root of a rotating beam specimen of mild steel after  $24 \times 10^6$  cycles at  $S_a \pm 39$  MPa. Circumferential V-notch, depth 1.3 mm, root radius 0.07 mm [11].

### 2.5.3 Small cracks, crack growth barriers, thresholds

It has been observed in laboratory experiments as well as in service that minute cracks were nucleated which stopped growing at a small crack length (Figure 2.7). Apparently, the cracks encountered a type of a crack growth barrier and could not grow any further. The barrier was a threshold for crack growth.

In the fifties, Frost et al. [11] studied so-called non-propagating fatigue cracks. He observed small fatigue cracks in notched specimens tested under a low cyclic load. Frost found small cracks which stopped growing at a crack length of some grain diameters. An example is shown in Figure 2.14. Frost did not observe a similar behavior on unnotched specimens, but for sharply notched specimens he concluded that small fatigue cracks could be initiated at stress amplitudes below the fatigue limit. His results for specimens with different stress concentrations are illustrated by the graph in Figure 2.15. For severe stress concentrations with large  $K_t$ -values,<sup>5</sup> crack initiation at low

<sup>5</sup>  $K_t$  is the stress concentration factor, an elastic concept discussed in Chapter 3. By definition  $K_t$  is the ratio of the peak stress in the notch and the nominal stress ( $K_t = S_{\text{peak}}/S_{\text{nom}}$ ).

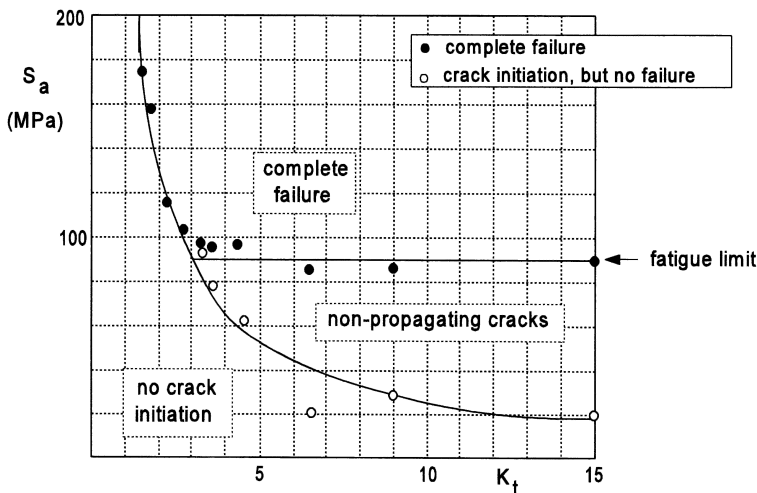


**Fig. 2.15** Observations of Frost [12] on non-propagating cracks as a function of  $K_t$ . Material: mild steel.

stress amplitudes could not be avoided because of the high peak stress at the root of the notch. However, the stress amplitudes were insufficient to maintain continuous crack growth and failure did not occur. As discussed before, initiation occurs at the material surface, where the restraint on cyclic slip is minimal. After some crack growth the crack tip stress field changes from plane stress at the free surface to plane strain deeper in the material. It implies an increased restraint on cyclic slip, and apparently crack arrest could occur as a consequence of insufficient cyclic slip. In this case, it is not really a material barrier that stops crack growth, but a change in the crack tip stress field. Such small cracks should be referred to as *mechanically short cracks*.

In the seventies and afterwards, it was recognized that non-growing microcracks can also occur in unnotched specimens. Again it means that crack nucleation occurs below the fatigue limit. The reasons for crack arrest, however, are different from those for the experiments of Frost. Several types of barriers to the growth of these cracks are possible. An example of a microstructural effect was already given in the discussion on Figure 2.5 with the grain boundaries as apparent barriers to a continuous growth of the microcrack. Although the grain boundaries did not stop microcrack growth in this case, it is possible that microcracks are nucleated in a grain, but cannot penetrate into the neighbouring grains, and thus remain arrested within that grain. Examples of other microstructural barriers are two-phase

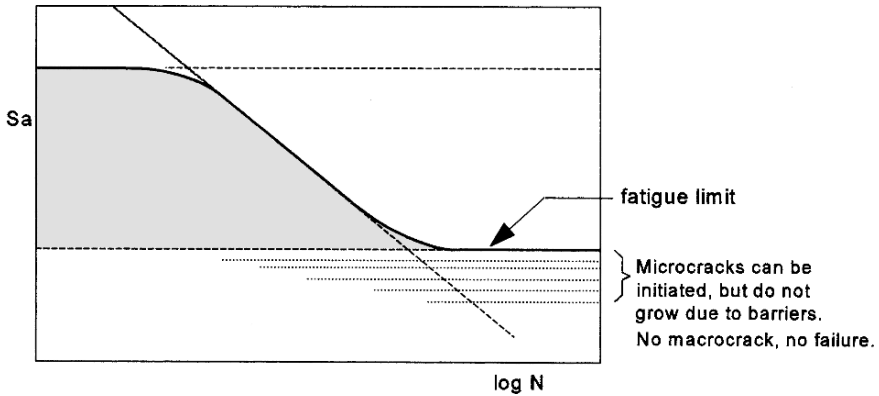
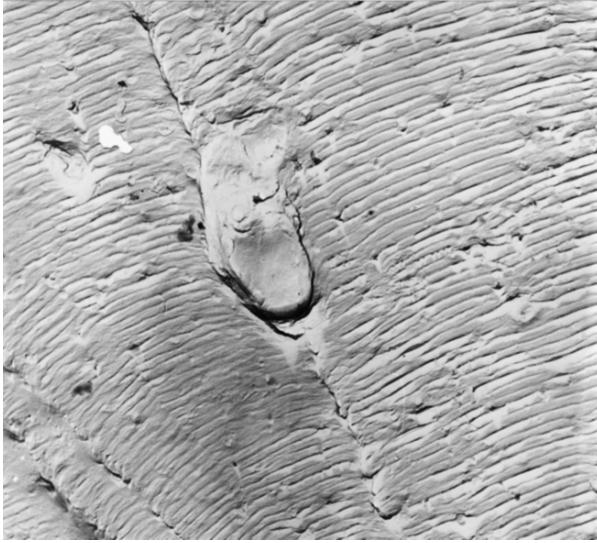


Fig. 2.16 Microstructurally small cracks below the fatigue limit of unnotched specimens.

boundaries, such as pearlite islands in low-carbon steel and  $\alpha/\beta$  interfaces in Ti-alloys. In general, the size of such non-growing cracks is in the order of the spacing between the microstructural barriers. Such cracks are referred to as *microstructurally small cracks*. The significance of material structural barriers is associated with their effect on cyclic slip at the tip of the microcrack.

Because of non-growing cracks below the fatigue limit, see Figure 2.16, the definition of the fatigue limit should be reconsidered. A frequently used definition says that the fatigue limit is the stress amplitude for which the fatigue life goes to infinity. Mathematically, the definition implies that the fatigue limit corresponds to the lower horizontal asymptote of the S-N curve. Another definition can now be postulated: the fatigue limit is the lowest stress amplitude for which crack nucleation is followed by crack growth until failure. Of course, this definition could also be formulated as the fatigue limit is the largest stress amplitude which does not lead to continuous crack growth until failure. The fatigue limit is thus recognized as a threshold for the growth of small cracks, and not as a threshold for crack nucleation. This observation is relevant for notch effects on fatigue discussed in Chapter 7.

It may be questioned if microscopically small barriers to slip can still have a significant effect on continuous crack growth, for instance, inclusions in the order of  $1\ \mu\text{m}$  (or in the sub-micron range). They can even be small compared to the size of microcracks. Although such inclusions will have a local effect on cyclic slip and local crack growth, the microcrack can grow around the inclusion. It thus will not be a barrier as a permanent threshold for further



**Fig. 2.17** Fatigue crack growth around an inclusion. Striation spacing about 0.5  $\mu\text{m}$ .

crack growth. Evidence for growing around inclusions has been shown for macrocracks in Al-alloys, see the example in Figure 2.17. Similar evidence for other materials is not abundant, but overcoming local barriers should also be expected to occur.

#### ***2.5.4 Number of crack nuclei***

It is an old and good question to ask why fatigue apparently occurs as a localized failure. Many times, a fatigue failure in service seems to be the result of the growth of a single fatigue crack only. An example of such a failure is shown in Figure 2.18. The fracture surface of a broken car axle suggests that the fatigue failure started at a single nucleation point. However, also for unnotched specimens tested in the laboratory the trend appears often to be valid. As said before, fatigue crack initiation is a surface phenomenon, but thousands of grains are found at the material surface of unnotched specimens. The question is whether the conditions for nucleation of a fatigue crack are similar for all surface grains? That is not true for several reasons. Nucleation depends on the occurrence of cyclic slip. However, the stress is not equal in all surface grains due to the anisotropy of the material (recall the discussion in Section 2.5.1). Moreover, the variation of the shape

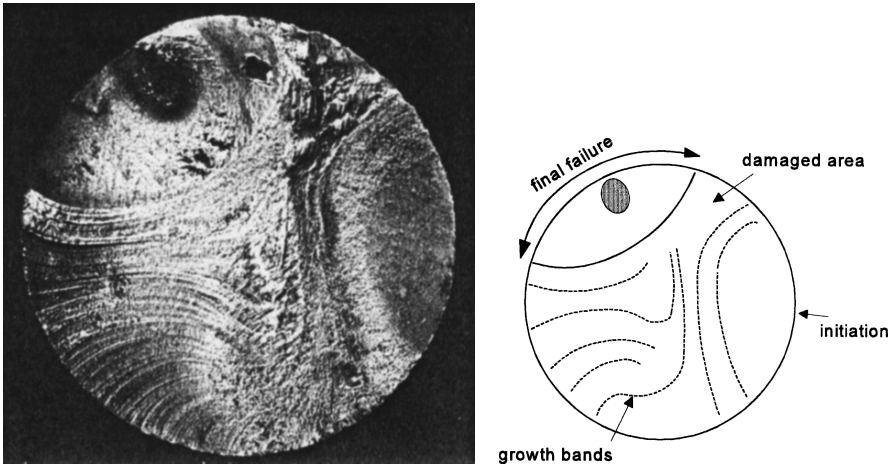


**Fig. 2.18** Fatigue fracture surface of a rear axle of a motor car, diameter 20 mm. The fatigue failure started as a single dominant fatigue crack.

and size of the grains also contributes to the inhomogeneity of the stress distribution on a microlevel. Furthermore, the orientation of the crystal lattice differs from grain to grain, which amplifies different possibilities for cyclic slip. If crack nucleation occurs at small inclusions near the free surface of the material, the size, shape and orientation of the inclusions is another source for differences between grains. Surface roughness can also contribute to some preferred locations for crack initiation. Nucleation of fatigue cracks in an unnotched specimen will therefore occur at a location where all combined conditions are most favorable for cyclic slip and crack nucleation. It seems to be reasonable that in a fatigue test only one dominant fatigue crack nucleus is detected on the fracture surface. This is particularly true if the cyclic stress level is close to the fatigue limit. The location of crack nucleation site may then be called the “weakest link” of the specimen.

Fatigue fracture surfaces as shown in Figure 2.18 suggest a single fatigue crack nucleus, but it is possible that more small fatigue cracks are present which are still too small to be seen on the fracture surface. They can also occur in different cross sections of a specimen without being linked up by the main crack. Furthermore, it should be recalled that the crack initiation period covers a relatively large part of the fatigue life, see Figure 2.7. It then is possible that a single crack has grown into the macrocrack growth period until complete failure while other cracks are still in the crack initiation period as a consequence of scatter of the local conditions for microcrack nucleation.

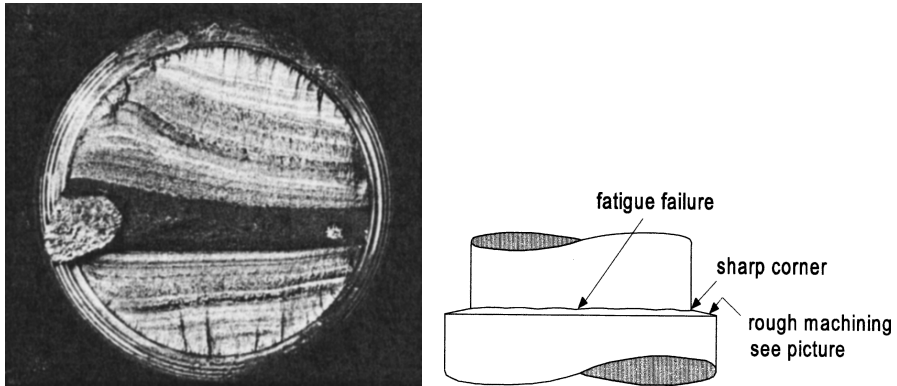


**Fig. 2.19** Fracture surface of a fatigue failure in the tiller of a sailing boat as a result of cyclic bending. Crack nucleation at several locations in the sharp corner edge. Overlap of crack nuclei produces lines in the crack growth direction.

The situation is different if the stress amplitude is high. The significance of microstructural thresholds becomes less important because they are more easily overcome at higher stress levels. As a result, more microcracks can develop successfully to a larger size. This has been observed, especially in Al-alloys. Stress levels between different grains in these alloys are relatively low because of the low elastic anisotropy (Section 2.5.1). Microscopic investigations on specimens of Al-alloys at relatively high stress levels have shown fairly large numbers of microcracks in different surface grains, e.g. [13, 14]. At a later stage linking up of these cracks occurred to form one single larger crack.

A high stress at the material surface is also obtained if sharp notches are present due to the high stress concentration. Crack initiation then is relatively easy and can occur at many places more or less simultaneously. Figure 2.19 shows the fatigue failure of a tiller of a sailing-vessel, which was primarily loaded by plane bending. Cracks initiated at the sharp corner of a diameter reduction, both at the top side and the lower side in Figure 2.19. The bending stress level was not high because a large amount of fatigue crack growth occurred as shown by the area of fatigue bands in Figure 2.19. As a consequence, the final failure in the last cycle of the fatigue life covers a relatively small area which is the horizontal dark band in the middle of Figure 2.19. However, the  $K_t$ -value at the root of the notch was extremely high due to the sharp corner, and thus crack nucleation occurred at many neighbouring locations. Overlapping of these cracks leads to the vertical lines in the crack growth direction. The lines are very small steps

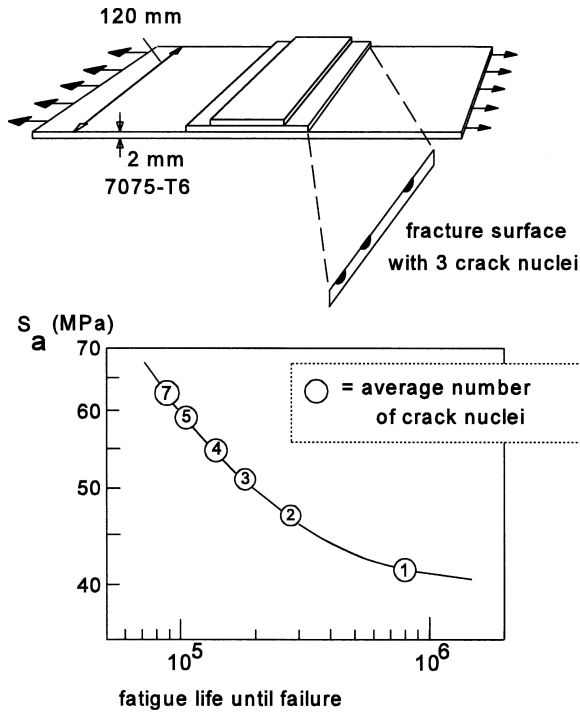
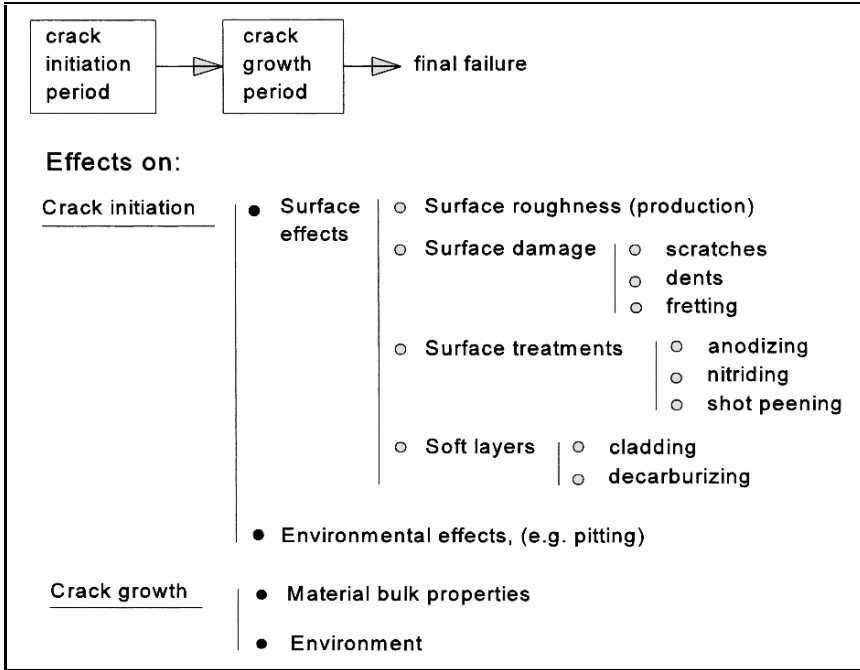


Fig. 2.20 The number of crack nuclei depends on the stress level [15].

in the fracture surface because the cracks initially started to grow in slightly staggered planes, see also Figure 2.33 to be discussed later.

Another illustrative example of multi-site crack nucleation is shown in Figure 2.20. The specimen consists of a sheet with adhesively bonded doublers. Fatigue cracks occur at the edge of the doubler because the doubler implies a local stress concentration which is further enhanced by additional bending of the specimen due to the doublers being present at one side of the sheet only. Tests were carried out at several stress levels to determine an S-N curve. All fracture surfaces were examined, and the number of visible crack nuclei were counted for each specimen. Average numbers of crack nuclei are indicated in the graph for different stress levels. Obviously the number of visible fatigue crack nuclei increases at higher stress levels, whereas only one nucleus was evident at a low stress level (the weakest link).

The above results confirm that crack nucleation at a low stress level is more problematic. It is indeed a threshold problem. At high stress levels the situation is entirely different because nucleation can occur anyway, and it can occur at several locations. A technically significant conclusion to be



**Fig. 2.21** Effects of the crack initiation and crack growth period.

drawn now is: If crack nucleation is problematic, scatter of fatigue properties must be expected. If crack nucleation is not problematic, scatter will be less sensitive to microstructural characteristics of the material, and thus scatter will be lower. This topic is addressed later in Chapter 12 on scatter of fatigue.

### 2.5.5 Surface effects

The discussion in Section 2.3 has indicated that fatigue in the crack initiation period is a surface phenomenon. It was also pointed out that the initiation period may cover the major part of the fatigue life until failure (Figure 2.7). As a consequence, various kinds of surface effects can be of great importance for the fatigue life. Surface effects include all conditions which can reduce the crack initiation period. In other words, they cover the phenomena which enhance the crack initiation mechanism. Several effects are mentioned in Figure 2.21. The list is not necessarily complete, but various well-known effects are listed. They are briefly discussed below while most effects are covered more extensively in later chapters. The purpose of the discussion

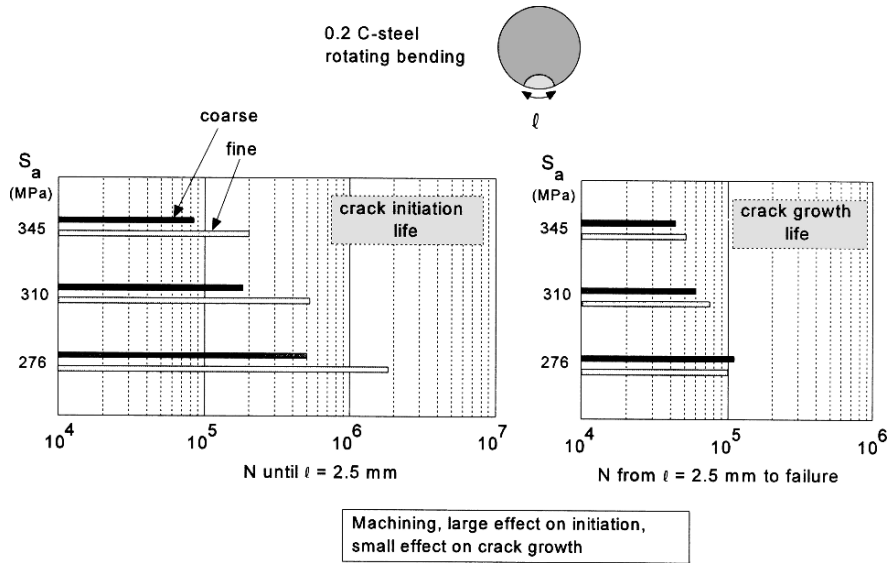


**Fig. 2.22** Effects of surface roughness on the crack initiation and crack growth period [16].

here is to reveal general aspects related to the fatigue process in terms of the crack initiation period and crack growth period.

Surface roughness and surface damage imply that the free surface is no longer perfectly flat. As a consequence, small sized stress concentrations along the material surface occur. Although the stress concentration will rapidly fade away from the surface, it is still significant for promoting cyclic slip and crack nucleation at the material surface. As an example, results of de Forest [16] are shown in Figure 2.22. He carried out rotating bending fatigue tests on specimens with two different surface roughnesses, coarse machining and fine machining. Rough machining causes deeper circumferential grooves than fine machining. De Forest periodically interrupted his tests to observe possible crack growth. He then defined the crack initiation period as the fatigue life until a circumferential crack length  $l = 2.5$  mm (0.1 inch) was reached, while the crack growth period covered the life from  $l = 2.5$  mm until failure. As shown by the test results at three different stress amplitudes, the crack initiation life is significantly shorter for rough machining if compared to fine machining, see the left-hand graph in Figure 2.22. However, according to the right-hand graph of Figure 2.22 the crack growth period is hardly affected by the surface roughness. A comparison of the two graphs in Figure 2.22 also reveals that the crack growth period is much shorter than the crack initiation period.

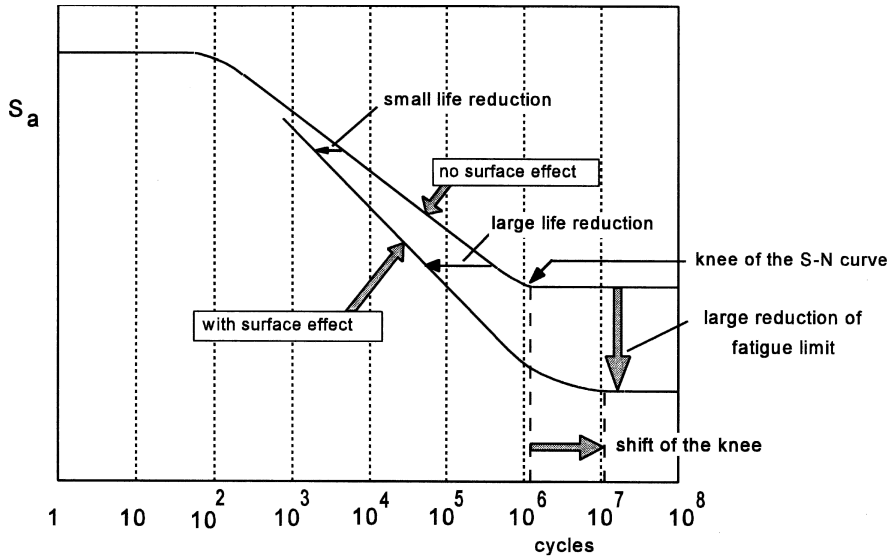


Fig. 2.23 Surface effects on the S-N curve. Both  $S_a$  and  $N$  are plotted on a logarithmic scale.

There is still another message in Figure 2.22. The crack initiation period significantly increases for a lower stress level, as should be expected. If the stress amplitude is reduced further to the fatigue limit, the crack initiation life becomes very large, confirming the threshold idea about the fatigue limit as discussed before. The crack growth period in Figure 2.22 also increases for a lower stress amplitude, but the effect is much smaller. This trend is generally observed for surface effects. The amplitude-dependent sensitivity is illustrated in Figure 2.23. The most detrimental consequence of an unfavorable surface effect is the large reduction of the fatigue limit. This is especially important for structural components designed for an infinite life, i.e. with all amplitudes in service below the fatigue limit. Unintentional surface damage, such as nicks and dents, can then be very harmful. The same is true for damage due to fretting, a phenomenon described in more detail in Chapter 15. The large reduction of the fatigue limit indicates that there is a range of stress amplitudes between the original  $S_f$  and the reduced  $S_f$  which can be harmful if surface damage is present. Without surface damage such fatigue cracks are not initiated, but with the assistance of surface damage cracks can be started and cause failure. Due to the relatively low stress amplitude, the crack growth life can be large. As a consequence, the inflection point of the S-N curve to the horizontal part (the so-called knee of

the S-N curve) occurs at a higher fatigue life as for the original S-N curve, see the shift of the knee in Figure 2.23.

If a design is made for a finite life, detrimental surface effects may be less important, specifically if the design life is short. Although surface damage can accelerate crack initiation, the high stress amplitude cycles can also generate crack nuclei early in the fatigue life, and the assistance of surface damage is less important for the initiation process. However, if the design life is large in numbers of cycles, the significance of adverse surface effects should be recognized. The high sensitivity for surface effects at low stress amplitudes and the relatively low sensitivity for surface effects at high stress amplitudes can lead to more scatter of the fatigue life at low amplitudes and less scatter at high amplitudes. This trend is generally observed in fatigue experiments. The trend was already mentioned in the previous section for similar reasons.

Shot peening is used as a remedy if fatigue problems are anticipated. Shot peening introduces plastic deformation in the surface layer of the material. As a result of the plastic deformation, residual compressive stresses are left in a thin surface layer. Because residual stresses do not affect cyclic shear stresses, cyclic slip may still occur. It even can lead to small microcracks, but crack growth is difficult. The residual compressive stresses reduce or prevent crack opening of the microcracks. As a result, the stress concentration at the crack tip is much lower and crack growth will be impeded. It may well be stopped completely. The residual compressive stress zone serves as a barrier for microcrack growth. There are many other ways to introduce residual stresses in the material of structural components. Residual stresses are very important for practical reasons. Possibilities for introducing residual stresses are discussed in Chapter 4.

The list in Figure 2.21 also refers to environmental effects. A brief discussion on this topic is presented in Section 2.5.7 and a more extensive treatment in a later chapter (Chapter 16).

### ***2.5.6 Crack growth and striations***

As discussed before, fatigue crack growth in the crack growth period is no longer affected by the material surface conditions. The crack growth is then a bulk material phenomenon. Usually the crack is growing perpendicular to the main principal stress. For uniaxial loading conditions in symmetric specimens, it implies that the crack growth direction is macroscopically

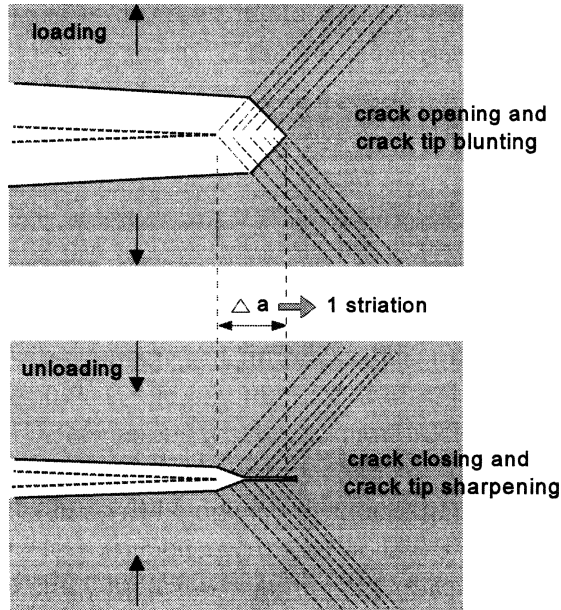


**Fig. 2.24** Crack extension in a single load cycle.

perpendicular to the loading direction. After the crack has grown away from the free surface, slip deformations will occur on more than one slip plane. Figure 2.24 gives a schematic visualization of a possible mechanism for crack extension in one load cycle. During loading the crack will be opened by crack tip plastic deformations, which in Figure 2.24 are supposed to occur on two symmetric slip systems. Stress analysis of a solid with a crack indicates that the slip zones in Figure 2.24 are indeed the zones with the maximum shear stress, both during loading and unloading. During loading the slip deformation will cause some crack extension. Also for these larger cracks, the crack extension implies decohesion, which should be associated with dislocations flowing into the crack tip, or being emitted by the crack tip. It also seems plausible that crack extension occurs in every successive load cycle in a similar way as sketched in Figure 2.24.

The slip deformations are not fully reversible due to strain hardening and other possible mechanisms. As illustrated by Figure 2.24, a ridge of microplastic deformation is left on the new upper and lower crack tip surfaces created in that particular cycle. These ridges are called “striations”, which can be observed on the fatigue fracture surface in the electron microscope. Although they were already observed long ago [17, 18] under the optical microscope, much better pictures were obtained in the electron

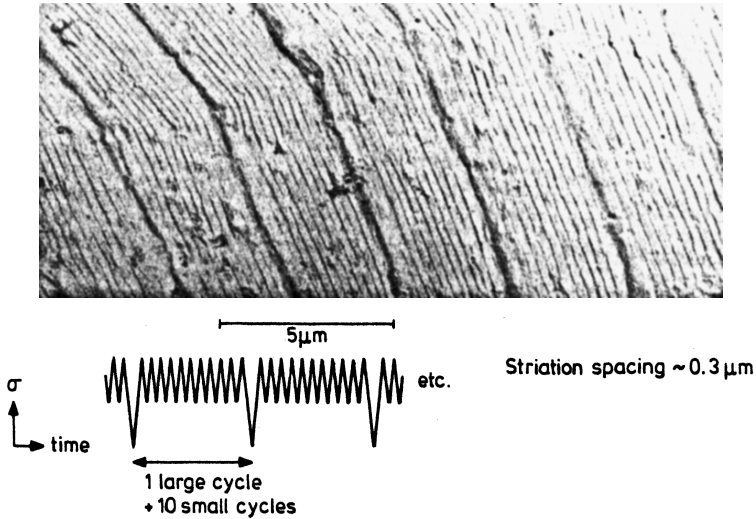


**Fig. 2.25** Correspondence between striations and load cycles during macrocrack growth in an Al-alloy sheet. (Picture National Aerospace Laboratory, NLR, Amsterdam)

microscope, originally in the Transmission Electron Microscope (TEM) and later abundantly in the Scanning Electron Microscope (SEM). An illustrative picture is shown in Figure 2.25. An aluminium alloy sheet specimen was loaded by a repetition of 10 small cycles and a single larger load cycle. There is a striking correspondence between the load history and the striation pattern. The 10 small cycles correspond to the smaller striation spacings, while the single larger cycle is responsible for the wider and more dark striation. Such pictures prove that crack extension did occur in each cycle of the load history. It also allows measurements of the crack growth rate (i.e. the crack extension per cycle) from such fractographs. The striation spacing for the small cycles in Figure 2.25 is about  $0.3 \mu\text{m}$  which thus corresponds to a crack growth rate of  $0.3 \mu\text{m}/\text{cycle}$ .

The occurrence of striations can give essential information to the analysis of failures occurring in service. First, if striations are observed, it shows that at least part of the failure occurred due to cyclic loads. Moreover, striations can give information about the crack growth direction and crack growth rate. Unfortunately, striations are not equally visible for all materials. Most useful observations have been obtained on aluminium alloys. However, striations were also observed on various types of steels, titanium alloys and some other alloys, but usually less abundantly and with less well-defined striations. If striations cannot be observed it should not be concluded immediately that fatigue did not occur.

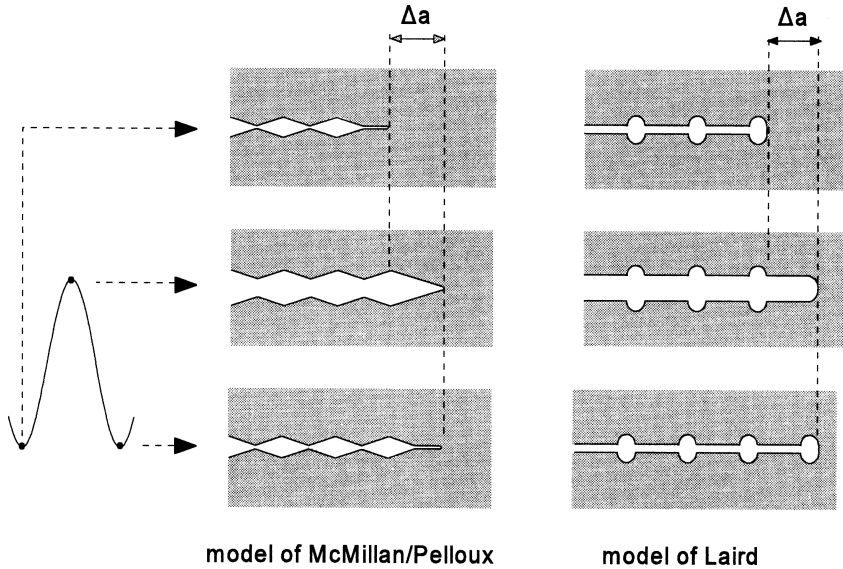


**Fig. 2.26** Two models for striation forming during fatigue crack growth [19, 20].

The geometry of the blunted crack tip in Figure 2.24 is a rather simple one. In reality it might be much more complex. The mechanism of fatigue crack growth at the crack tip has been a subject of much speculation in the literature. Two well-known models are presented in Figure 2.26. Both models create one striation in each cycle, but the crack tip blunting and crack tip resharpening is different for the two models. The first model by McMillan and Pelloux [19] is similar to the sketch in Figure 2.24. It implies that the crack tip upon unloading is closed, starting at the crack tip. However, in the model of Laird [20] closing of the crack starts behind the crack tip, which creates a kind of an ear marking at the end of the crack extension in a cycle. Because the formation of striations is a result of cyclic plasticity, it is very well possible that the striation geometry depends on the type of material. The McMillan–Pelloux model was developed for Al-alloys, while Laird supported his model with observations for pure metals.

Microscopic research studies on the mechanism of crack extension under cyclic loading have received much attention for years, but some major problems were encountered. Fatigue cracks observed at the free surface of the material do not necessarily show the same behavior as the crack front inside the material. At the free surface, the deformation restraint on cyclic slip is different from the restraint inside the material. Secondly, at the interior of the material, observations on striations can be made only after opening of

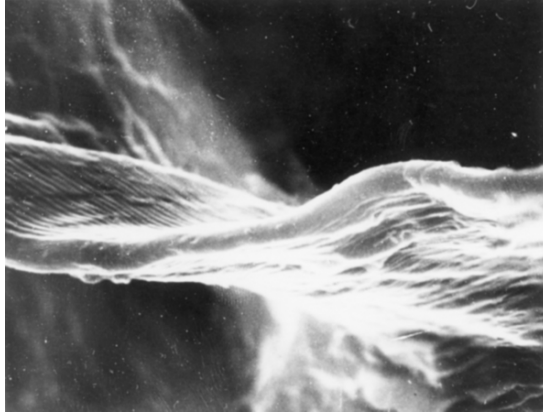


**Fig. 2.27** Casting of a fatigue crack (2024-T3 aluminium alloy, width of picture 16  $\mu\text{m}$ ). Technique developed by Quinton Bowles [21]. Curved crack front and striations at both sides of the casting.

the fatigue crack. It gives the final topography, but not the situation during the dynamic process of crack extension and crack tip closure. Moreover, the dimensions of details of striations are in the sub-micron range where observations are difficult. An interesting technique was developed by Bowles [21]. He used a vacuum infiltration method, which implies that the crack at any selected load can be filled with a plastic. The crack serves as a mould. After hardening of the plastic, the material of the aluminium specimen is removed by a chemical solvent. A casting of the crack is then obtained, which can be studied in the SEM. A picture is shown in Figure 2.27. It shows striations of the upper and lower side of the fatigue crack. More important, it shows that the tip of the fatigue crack is not sharp but rounded (estimated radius 0.4  $\mu\text{m}$ ), and the crack front is not a straight line. The latter observation was already confirmed by Figure 2.25. The infiltration technique until now has been applied to Al-alloys only. The method cannot be used for materials where chemical removal of the specimen material is difficult which applies to steel. However, knowledge about the geometry of the crack front is significant for the justification of applying fracture mechanics to predictions on fatigue crack propagation, the subject of Chapters 8 and 11.

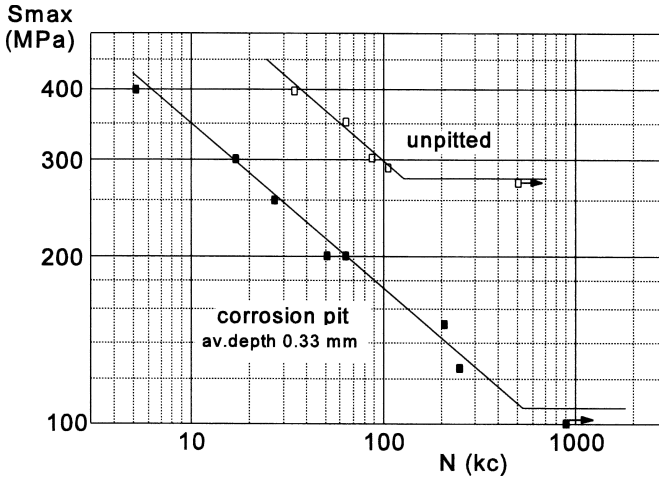


**Fig. 2.28** The effect of a corrosion pit on the S-N curve of unnotched specimens of an Al-alloy [22].

### 2.5.7 Environmental effects

As indicated in Figure 2.21, the environment can affect both crack initiation and crack growth. It should be pointed out that there is a difference between fatigue of corroded specimens in a non-aggressive environment, and fatigue of initially undamaged specimens in a corrosive environment. The first case is illustrated by Figure 2.28. Unnotched specimens of a notch sensitive Al-alloy (7075-T6) were provided with a corrosion pit to a depth of approximately 0.3 mm. These specimens were then used to obtain an S-N curve. For the material used, such a corrosion pit is severe surface damage, also because the shape of a corrosion pit represents a significant stress raising geometry. As shown by the S-N curves in Figure 2.28 the fatigue life at high stress amplitudes is reduced about six times. But the most dramatic effect is the reduction of the fatigue limit  $S_f$ . Without the corrosion pits  $S_f$  is 275 MPa, whereas it is only 110 MPa if there is a corrosion pit. It confirms a basic idea of Figure 2.23. Stress amplitudes below the original fatigue limit are unable to create a fatigue crack. However, with the corrosion pit, cracks can be initiated and cause failure. Figure 2.28 also illustrates the shift of the knee already defined in Figure 2.23. A similar effect of corrosion pits on the S-N curve of a martensitic 12% Cr-steel for turbine blades was found by Zhou and Turnbull [23].

In general, corrosion fatigue refers to acceleration of crack initiation and crack growth under the combined action of fatigue and corrosion. The

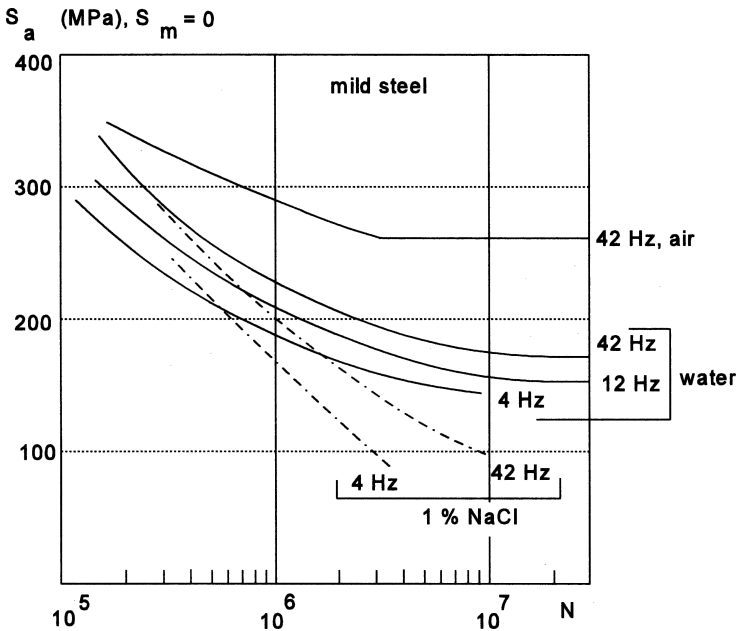
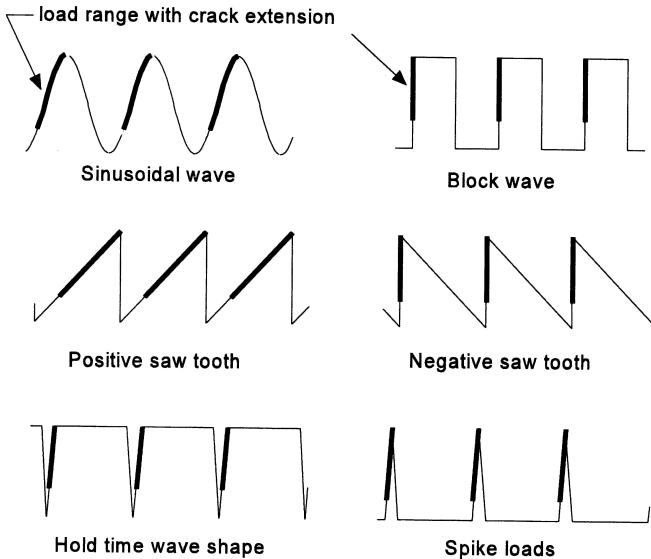


Fig. 2.29 The effect of environment and load frequency on the S-N curve of unnotched mild steel specimens [24].

acceleration should be associated with some contribution of a corrosive environment to the fatigue fracture mechanism. The S-N curves in Figure 2.29 illustrate a large effect. Endo and Miyao [24] carried out rotating bending tests on unnotched mild steel specimens in three environments; air, tap water and salt water. A dramatic effect on the S-N curve is observed. Again, a large reduction of the fatigue limit is evident. Although the effect at a high stress amplitude is still significant, it is much smaller, again in agreement with the trends shown in Figure 2.23. Unfortunately, the occurrence of a fatigue limit in salt water is not indicated by the curves in Figure 2.29. Apparently the salt water corrosion is successful in assisting the crack initiation and subsequent crack growth at very low stress amplitudes.

The results in Figure 2.29 also show that the frequency of the fatigue load has a systematic effect both in tap water and in salt water, compare the results for 42 Hz and 4 Hz. Because corrosion is a time dependent phenomenon, a frequency effect has to be expected. Actually, this effect is disturbing if structures are operating in a marine environment (ships, offshore structures) where load frequencies can be very low.

The effect of corrosion on crack nucleation and crack growth is a difficult phenomenon to be described in physical and electro-chemical terms. It may



**Fig. 2.30** Basic wave shapes of a cyclic load.

well be possible that crack extension is promoted by an aggressive agent at the crack tip. Because crack extension is decohesion of the material, foreign ions of the environment can weaken the cohesive strength of the material in some way. It has also been thought that some resolving of the material at the crack tip can occur. The mechanism will depend on the specific combination of the material and the environment. Aspects of cyclic crack tip plasticity, crack extension and environmental contributions are a difficult problem to study in physical details. One important aspect has to be mentioned here. If the load frequency has a significant effect, because of some time dependent corrosion mechanism, it should be expected that the wave shape of the load cycle can also have an effect on crack growth. In fatigue tests, the wave shape usually is sinusoidal, but in service it can be highly different. Several basic wave shapes are shown in Figure 2.30. Even if the load frequency of these wave shapes is the same in numbers of cycles per minute, corrosion fatigue does not necessarily occur at the same rate. It should be recognized that crack extension as a result of crack tip plasticity occurs during loading to  $S_{\max}$  as a progressive process. It is not just a crack length jump  $\Delta a$  at the moment that  $S_{\max}$  is reached. Crack extension occurs in the period before  $S_{\max}$  is reached. In this period a corrosive environment can enhance the decohesion, and thus amplify the crack extension. The short period of the crack extension process becomes the significant variable. The period is indicated as a black line in the

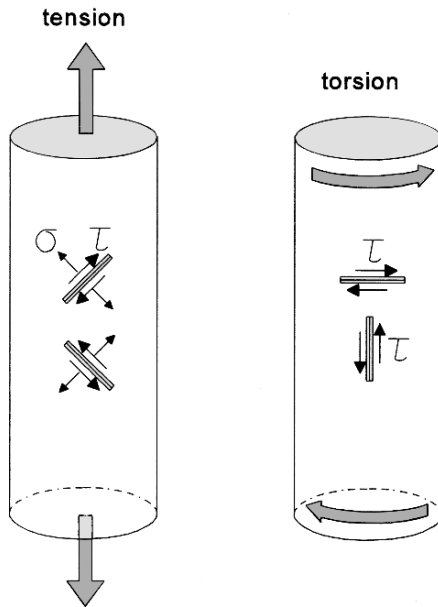


**Fig. 2.31** Slip planes with maximum shear stress.

wave shapes shown in Figure 2.30. It then is remarkable to see a significantly different period for the positive and the negative saw tooth wave shape. The loading rate of the positive saw tooth wave is relatively low. Crack extension occurs during a large part of the load cycle period. By contrast, the loading rate is high for the negative saw tooth wave shape. Crack extension by crack tip plasticity occurs in a very small fraction of the cyclic load period. As a consequence, not much time is available for a corrosive contribution to the crack extension process. A much lower effect on the crack growth rate should be expected. Relevant experiments were carried out by Barsom [25] on a high-alloy steel tested in salt water at 0.1 Hz. It turned out that crack growth for the positive saw tooth wave was about three times faster than for the negative saw tooth wave (see also Chapter 16).

### ***2.5.8 Cyclic tension and cyclic torsion***

As discussed before, cyclic slip is essential for microcrack nucleation and early microcrack growth. Crack nucleation in an unnotched specimen will now be considered for two loading cases: (1) cyclic tension, and (2) cyclic torsion, see Figure 2.31. Under cyclic tension the maximum shear stress



(a) Spiral crack due to cyclic torsion. No macroplastic deformation

(b) Same fatigue failure of (a). Arrow indicates starting point of fatigue crack at a surface pit

**Fig. 2.32** Fatigue failure of drive shaft of a scooter starting at surface damage.

occurs on planes at an angle of  $45^\circ$  with respect to the longitudinal axis. Under cyclic torsion, planes with a maximum shear stress are perpendicular and parallel to the longitudinal axis. An important difference between the two loading systems is that the plane of maximum shear stress in the tension case also carries a normal stress component ( $\sigma = \tau$ ). For cyclic torsion, however, this normal stress component on that slip plane is zero. As long as the initiation is still a matter of cyclic slip in a single surface grain, the two cases are essentially different. In the cyclic tension case the normal stress tries to open the microcrack and that will enhance the transition from cyclic slip into microcrack growth along the slip band. However, under cyclic torsion this crack opening effect is absent. Microscopical investigations have shown that nucleation in a slip band under cyclic torsion is problematic if the load amplitude is low, i.e. close to the fatigue limit. But for higher amplitudes above the fatigue limit, microcracks under cyclic torsion are generated which then grow further in a direction perpendicular to the main principal stress. In the cylindrical bar of Figure 2.31 this direction occurs at an angle of  $45^\circ$  with the axis of the bar. As a consequence, cracks in a round axle under cyclic torsion grow as a spiral around the surface of the axis. An example is shown in Figure 2.32, a drive shaft of a scooter, broken by torsional fatigue. The fatigue failure started at a surface damaging pit.

## 2.6 Characteristic features of fatigue failures

Several characteristic features of fatigue fracture surfaces have been discussed in previous sections. They are repeated here together with some more typical aspects. The characteristic features are significant in

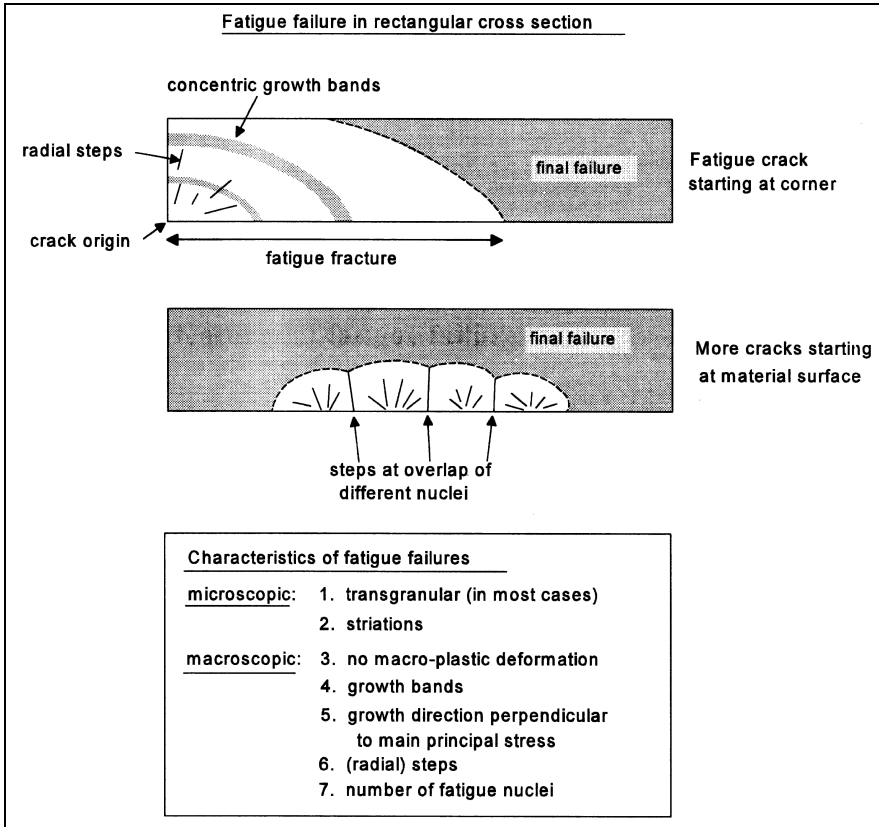


**Fig. 2.33** Survey of characteristic features of fatigue fracture surfaces.

failure analysis in order to distinguish between fatigue failures, static failure, including brittle failures, stress corrosion failures and creep failures. Moreover, if a fracture surface indicates that a failure is due to fatigue, it may well be possible to arrive at more details about the service fatigue load history. Examinations of fatigue failures of laboratory specimens can also give worthwhile information to validate fatigue prediction models.

The characteristics of a fatigue fracture are divided into two groups, microscopic features and macroscopic features, see Figure 2.33. It may be noted here that papers and test reports on fatigue experiments should always include a description of the fracture surfaces. Without these observations the discussion of the test results is inadmissibly incomplete.

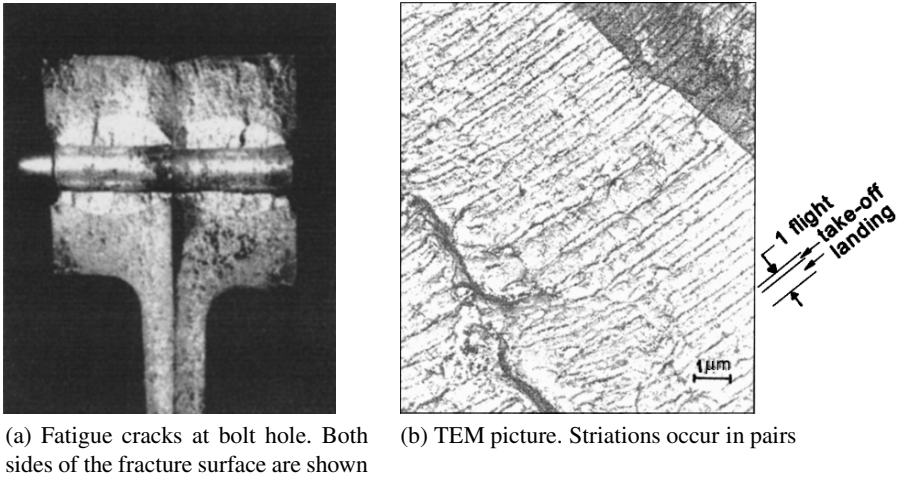


**Fig. 2.34** Striations in pairs on a fatigue fracture in a flap beam of an aircraft [8].

## 2.6.1 Microscopic characteristics

### (1) Transgranular crack growth

Fatigue cracks in almost all materials are growing along a transgranular path, i.e. through the grains. They do not follow the grain boundary, contrary to stress corrosion cracks and creep failures. Because fatigue crack growth is a consequence of cyclic slip, it is not surprising that fatigue crack prefers to grow through the grains. Restraint on slip exerted by the grain boundaries is minimal inside the grains. The transgranular character can easily be observed on microscopic samples in the optical microscope.

### (2) Striations

As discussed before, striations are remnants of microplastic deformations of individual load cycles, see Figures 2.24 to 2.27. The striations indicate the cyclic nature of the load history. The visibility of striations depends on the type of material and the load history as well. If striations cannot be observed, it need not imply that the failure is not due to fatigue.

An example of striations on a failure occurring in service is given in Figure 2.34. A flap beam of an aircraft failed during landing due to fatigue at a bolt hole (Figure 2.34a). The electron microscope revealed that striations occurred in pairs with a larger and a smaller striation spacing respectively (Figure 2.34b). The flap beam was loaded significantly twice in each flight, viz. by a large load during landing (flaps fully out) causing the wider

striation, and a lower load during take off (flaps only partly out) causing the smaller striation. It implies that each pair of striations corresponds to a single flight. The number of flights could thus be counted on the larger part of the fatigue fracture surface. It corresponded to a crack growth life of approximately 5000 flights. This example of striations also confirms that crack propagation occurs cycle-by-cycle. It also indicates that the information on crack growth in the component can be useful in order to assess periodic inspections for fatigue cracks and thus ensure safe flights.

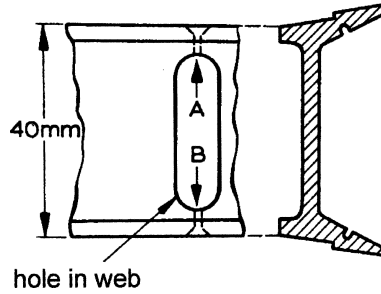
### ***2.6.2 Macroscopic characteristics***

Macroscopic characteristics of a fatigue failure can be observed with the naked eye. However, it always should be advised to look also with a small magnifying glass with a magnification of 6 to 8 $\times$ . It is often surprising how many details then can be observed, e.g. small crack nuclei, sites of crack nuclei, surface damage causing a crack nucleus, etc., details which escape visual observations by eye but which may be significant for the evaluation of the fatigue problem. Moreover, some details are sometimes overlooked at larger magnification in the electron microscope.

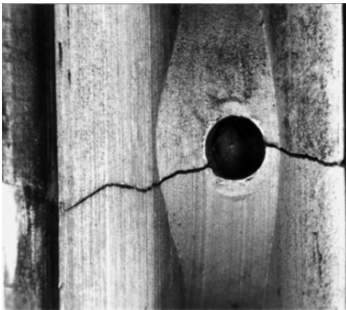
#### ***(3) No macroplastic deformation and a flat fatigue fracture surface***

The fracture surface of a fatigue failure usually shows two different parts:

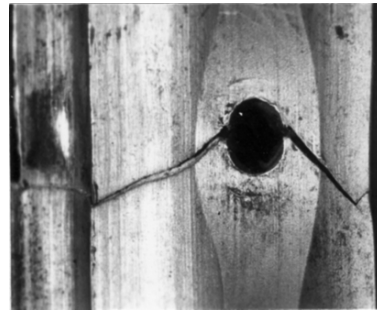
- (i) The real fatigue failure caused by fatigue crack growth (see Figure 2.33) is characterized by practically no macroplasticity. Because fatigue is a result of microplastic deformations, which are largely reversed in each cycle, it is not surprising that macroscopic deformations appear to be absent. For the major part of the fatigue life, the crack can hardly be seen on the material surface. Crack detection during service inspections may become problematic. Various NDI techniques have been developed for that purpose.
- (ii) The second part of the fracture surface is caused by the final failure in the last load cycle. It occurs if the remaining uncracked cross section of the material can no longer carry the maximum load of the load cycle. In general, the final failure can be considered to be a quasi-static failure. It will exhibit macroplastic deformation, depending on the ductility of the material. The difference between a fatigue failure without visible plastic deformation and a static failure with visible plastic deformation is illustrated by two pictures of a failure in a light alloy helicopter blade



(a) Cross section with hole in the web of the spar of a helicopter blade



(b) View of fatigue failure according to arrow A. No macroplastic deformation. Both parts fit well together



(c) View of static failure according to arrow B. Macroplastic deformation, ovalized hole, necking at right edge

**Fig. 2.35** Difference between a fatigue failure and a static failure, both occurring in the same spar of a helicopter blade. The fatigue failure of (b) caused the static failure of (c). Hole diameter 3 mm.

in Figure 2.35. The blade separated from the helicopter during starting procedures before takeoff; the helicopter capsized, but no fire and no fatalities. Blade failure occurred in a section with a lightening hole in the spar of the blade with a rivet hole at the top and the bottom side, see Figure 2.35a. The failure in section A did not show any macroplastic deformation as can be seen in Figure 2.35b where the two sides of the failure still fit nicely together. However, such a nice fit was not possible for the other rivet hole, see Figure 2.35c, because of macroplastic deformation visible by hole ovality and necking at the edges.

#### (4) Growth bands

Fatigue failures obtained in service often show growth bands which are visible with the naked eye, see Figure 2.36, and also Figures 2.18 and 2.19. The bands are also referred to as oyster-shell markings or beach markings. The bands indicate how the crack has been growing. The different colours

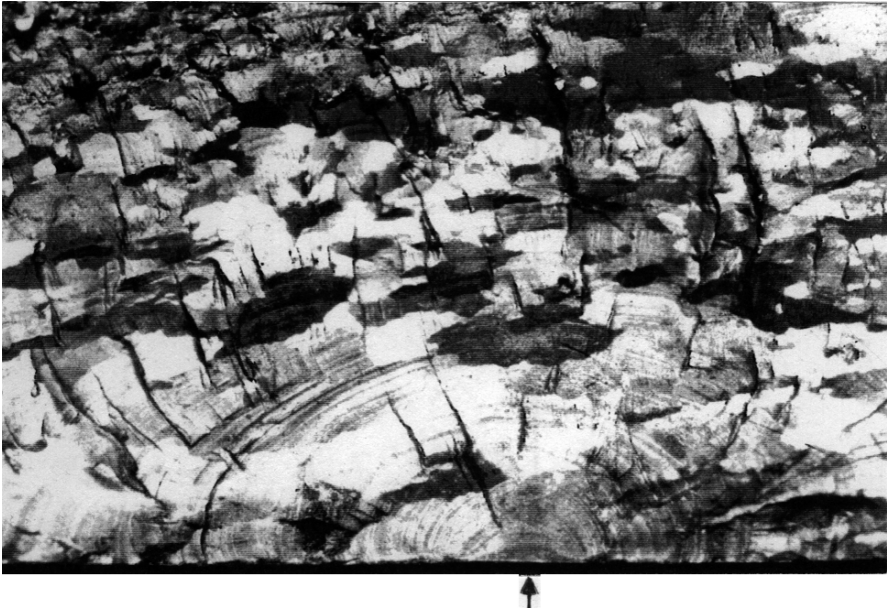


**Fig. 2.36** Fracture surface of a light metal compressor blade. The fatigue failure started at the lower surface (arrow). Top to bottom of picture: 3 mm.

are associated with variations of the stress level of the cyclic load. This is illustrated by a picture obtained in some elementary experiments, see Figure 2.37. Blocks of cycles with two different  $S_{\max}$ -values were applied alternately to specimens with edge notches. Approximately quarter circular cracks have grown from both edge notches. The dark bands were caused by the cycles with the higher  $S_{\max}$ . Different degrees of corrosive attack can also cause bands, especially if cracks are dormant for certain periods.

*(5) The growing direction, perpendicular to the main principal stress*

As discussed before, fatigue cracks are growing in a direction perpendicular to the main principle stress (provided the crack growth rate is not very high). Depending on the geometry of the component, it implies for a cyclic tension load that crack growth will be perpendicular to the loading direction. For cyclic torsion the crack in a circular bar will occur at  $45^\circ$  with the longitudinal axis. An example of the spiral crack growth was given before, see Figure 2.32.

A noteworthy exception to the “perpendicular” crack growth is observed in some materials, e.g. Al-alloys and some steels. The growing fatigue crack at the material surface exhibits so-called shear lips, see Figure 2.38, at an

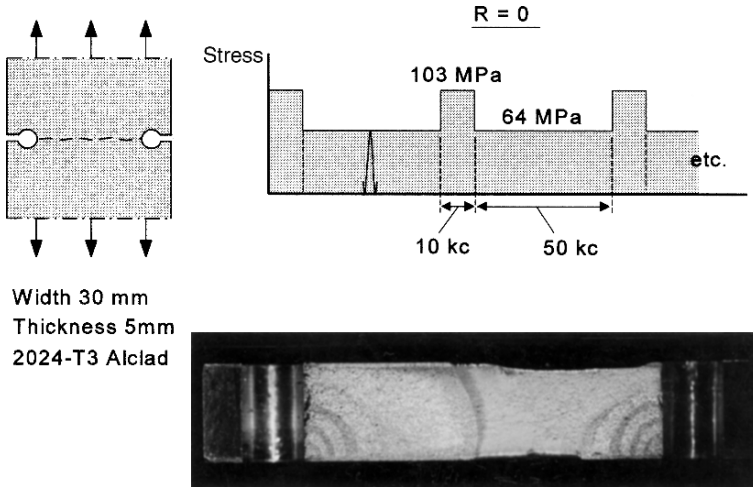


Fig. 2.37 Crack growth bands on the fracture surface of an aluminium alloy specimen with two side notches ( $K_t = 2.85$ ) [27].

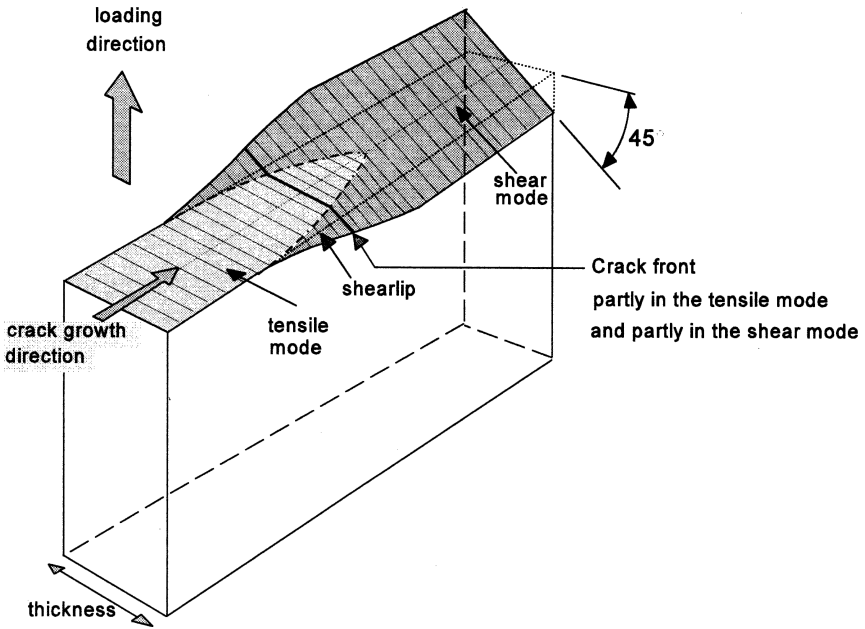


Fig. 2.38 Transition from crack growth in the tensile mode to the shear mode.

angle of approximately  $45^\circ$  with the central part of the crack front. The shear lip width increases during faster crack growth until they cover the full thickness. The shear lips start at the material surface, and in fact it should

be considered to be a free surface phenomenon. The possibilities for plastic deformation at the location where the crack front meets the free surface are less restrained than at mid-thickness. It apparently allows plastic shear deformations which promote the formation of shear lips. These shear lips are of a similar nature as shear lips observed on the fracture surface of static failures along the free surface edges. For crack growth predictions, the shear lips could be a problem. This question is considered in Chapter 11. Shear lips also imply that microscopic observations on the material surface are not necessarily characteristic for the fatigue mechanism below the material surface.

#### *(6) Radial steps and the number of fatigue crack nuclei*

These two characteristics have already been discussed in Section 2.5.4. The radial steps as schematically indicated in Figure 2.33, are also visible in Figure 2.36 where the deformation texture of the forged alloy promotes crack growth on planes in slightly different directions. This is also confirmed by the dark and light areas, which are reflections of crack growth in different grains. The radial steps in Figure 2.19 were already mentioned previously.

## **2.7 Main topics of the present chapter**

This section should not be considered to be a summary of the previous sections. The purpose is to present a list of the major findings, which are significant for applications in subsequent chapters.

1. The fatigue mechanism in metallic materials should basically be associated with cyclic slip and the conversion into crack initiation and crack extension. Details of the mechanism are dependent on the type of material.
2. The fatigue life until failure comprises two periods, the crack initiation period and the crack growth period. The crack initiation period includes crack nucleation at the material surface and crack growth of microstructurally small cracks. The crack growth period covers crack growth away from the material surface.
3. In many cases the crack initiation period covers a relatively large percentage of the total fatigue life.
4. Fatigue in the crack initiation period is a surface phenomenon, which is very sensitive to various surface conditions, such as surface roughness, fretting, corrosion pits, etc.

5. In the crack growth period, fatigue is depending on the crack growth resistance of the material and not on the material surface conditions.
6. Microstructurally small cracks can be nucleated at stress amplitudes below the fatigue limit. Crack growth is then arrested by microstructural barriers. The fatigue limit as a threshold property is highly sensitive to various surface conditions. At high stress amplitudes, and thus relatively low fatigue lives, the effect of the surface conditions is much smaller.
7. In view of possible effects during the crack initiation period, it can be understood that scatter of the fatigue limit and large fatigue lives at low stress amplitudes can be large, whereas scatter of lower fatigue lives at high amplitudes will be relatively small.
8. Aggressive environments can affect both crack initiation and crack growth. The load frequency and the wave shape are then important variables.
9. Predictions on fatigue properties are basically different for the crack initiation life and for the crack growth period.
10. The various characteristics of fatigue fractures can be understood in terms of crack initiation and crack growth mechanisms. These characteristics are essential in failure analysis, but they are also relevant to understand the significance of technically important variables of fatigue properties.

## References

1. Ewing, J.A. and Humfrey, J.C.W., *The fracture of metals under repeated alternations of stress*. Phil. Trans. Roy. Soc., Vol. A200 (1903), pp. 241–250.
2. Bullen, W.P., Head, A.K. and Wood, W.A., *Structural changes during the fatigue of metals*. Proc. Roy. Soc., Vol. A216 (1953), p. 332.
3. Forsyth, P.J.E., *The Physical Basis of Metal Fatigue*. Blackie and Son, London (1969).
4. Blom, A.E., Hedlund, A., Zhao, W., Fathalla, A., Weiss, B. and Stickler, R., *Short fatigue crack growth in Al 2024 and Al 7475*. Behaviour of Short Fatigue Cracks, Symp., September 1985, Sheffield. EGF 1, MEP (1986), pp. 37–66.
5. Cummings, H.N., Stulen, F.B. and Schulte, W.C., *Tentative fatigue strength reduction factors for silicate-type inclusions in high-strength steels*. Proc. ASTM, Vol. 58 (1958) pp. 505–514.
6. Murakami, Y., Takada, M. and Toriyama, T., *Super-long life tension-compression fatigue properties of quenched and tempered 0.46% carbon steel*. Int. J. Fatigue, Vol. 20 (1998), pp. 661–667.
7. Kung, C.Y. and Fine, M.E., *Fatigue crack initiation and microcrack growth in 2024T4 and 2124-T4 aluminum alloys*. Metall. Trans. A, Vol. 10A (1979), pp. 603–610.

8. Schijve, J., *The practical and theoretical significance of small cracks. An evaluation.* Fatigue 84. Proc. Int. Conf. on Fatigue Thresholds, Birmingham. EMAS (1984), pp. 751–771.
9. Forrester, P.G., *Fatigue of Metals.* Pergamon Press, Oxford (1962).
10. Ransom, J.T., *The effect of inclusions on the fatigue strength of SAE 4340 steels.* Trans. Am. Soc. Metals, Vol. 46 (1954), pp. 1254–1269.
11. Frost, N.E. and Phillips, C.E., *Studies in the formation and propagation of cracks in fatigue specimens.* Proc. Int. Conference on Fatigue of Metals, London, September 1956. The Institution of Mechanical Engineers (1956), pp. 520–526.
12. Frost, N.E., Marsh, K.J. and Pook, L.P., *Metal Fatigue.* Clarendon, Oxford (1974).
13. Kung, C.Y. and Fine, M.E., *Fatigue crack initiation and microcrack growth in 2024T4 and 2124-T4 aluminum alloys.* Metall. Trans. A, Vol. 10A (1979), pp. 603–609.
14. Sigler, D., Montpetit, M.C. and Haworth, W.L., *Metallography of fatigue crack initiation in an overaged highstrength aluminium alloy.* Metall. Trans. A, Vol. 14A (1983), pp. 931–938.
15. Schijve, J., *Fatigue predictions and scatter.* Fatigue Fract. Engng. Mater. Struct., Vol. 17 (1994), pp. 381–396.
16. de Forest, A.V., *The rate of growth of fatigue cracks.* J. Appl. Mech., Vol. 3 (March 1936), pp. A-23 to A-25.
17. Zappfe, C.A. and Worden, C.O., *Fractographic registrations of fatigue.* Trans. Am. Soc. Metals, Vol. 43 (1951), pp. 958–969.
18. Forsyth, P.J.E. and Ryder, D.A., *Some results of the examination of aluminium alloy specimen fracture surfaces.* Metallurgia, Vol. 63 (1961), pp. 117–124.
19. McMillan, J.C. and Pelloux, R.M.N., *Fatigue crack propagation under program and random loading.* Fatigue Crack Propagation, ASTM STP 415 (1967), pp. 505–535.
20. Laird, C., *The influence of metallurgical structure on the mechanisms of fatigue crack propagation.* Fatigue Crack Propagation, ASTM STP 415 (1967), pp. 131–180.
21. Bowles, C.Q. and Schijve, J., *Crack tip geometry for fatigue cracks grown in air and vacuum.* Advances in Quantitative Measurement of Physical Damage. ASTM STP 811 (1983), pp. 400–426.
22. Scheerder, C., *The danger of single corrosion pits with respect to fatigue.* Master Thesis, Faculty of Aerospace Engineering, Delft University of Technology (1992).
23. Zhou, S. and Turnbull, A., *Influence of pitting on the fatigue life of a turbine blade steel.* Fatigue Fract. Engng. Mater. Struct., Vol. 22 (1999), pp. 1083–1093.
24. Endo, K. and Miyao, Y., *Effects of cycle frequency on the corrosion fatigue strength.* Bull. Japan Soc. Mech. Engrs., Vol. 1 (1958), pp. 374–380.
25. Barsom, J.M., *Effect of cyclic stress form on corrosion fatigue crack propagation below  $K_{Isc}$  in a high yield strength steel.* Corrosion Fatigue: Chemistry, mechanics and Microstructure, O.F. Devereux, A.J. McEvily and R.W. Staehle (Eds.), Vol. NACE-2. National Association of Corrosion Engineers, Houston (1972), pp. 424–436.
26. Broek, D., *Accident investigation.* Report of the National Aerospace Laboratory NLR, Amsterdam.
27. Schijve, J., *Fatigue crack propagation in light alloys.* National Aerospace Laboratory NLR, Amsterdam, Report M.2010 (1956).

#### *Some general references*

28. Murakami, Y., *Metal Fatigue: Effects of Small Defects and Nonmetallic Inclusions.* Elsevier (2002).

29. Suresh, S., *Fatigue of Materials*, 2nd edn. Cambridge University Press, Cambridge (1998).
30. Miller, K.J., *The three thresholds for fatigue crack propagation*. ASTM STP 1296, R.S. Piascik, J.C. Newman, and N.E. Dowling (Eds.). ASTM (1997), pp. 267–286.
31. *Fatigue and Fracture*. American Society for Materials, Handbook Vol. 19, ASM International (1996).
32. Carpinteri, A., *Handbook of Fatigue Cracking – Propagation in Metallic Structures*. Elsevier, Amsterdam (1994).
33. *Fractography*. American Society for Materials, Handbook Vol. 12. ASM International (1987).
34. Ritchie, R.O. and Lankford, J. (Eds.), *Small Fatigue Cracks*. Proc. 2nd Engineering Foundation Int. Conf., 1986. The Metallurgical Society (1986).
35. Miller, K.J. and de los Rios, E.R. (Eds.), *The Behaviour of Short Fatigue Cracks*. EGF Publication 1, Mechanical Engineering Publications, London (1986).
36. Fuchs, H.O. and Stephens, R.I., *Metal Fatigue in Engineering*. John Wiley & Sons (1980).
37. Klesnil, M. and Lukás, P., *Fatigue of Metallic Materials*, 2nd edn. Elsevier, Amsterdam (1992).
38. Fong, J.T. (Ed.), *Fatigue Mechanisms*. ASTM STP 675 (1979).
39. Kocanda, S. *Fatigue Failure of Metals*. Sijthoff & Noordhoff (1978).